INFORMATION TO USERS

This manuscript has been reproduced from the microfilm master. UMI films the text directly from the original or copy submitted. Thus, some thesis and dissertation copies are in typewriter face, while others may be from any type of computer printer.

The quality of this reproduction is dependent upon the quality of the copy submitted. Broken or indistinct print, colored or poor quality illustrations and photographs, print bleedthrough, substandard margins, and improper alignment can adversely affect reproduction.

In the unlikely event that the author did not send UMI a complete manuscript and there are missing pages, these will be noted. Also, if unauthorized copyright material had to be removed, a note will indicate the deletion.

Oversize materials (e.g., maps, drawings, charts) are reproduced by sectioning the original, beginning at the upper left-hand corner and continuing from left to right in equal sections with small overlaps.

ProQuest Information and Learning
300 North Zeeb Road, Ann Arbor, MI 48106-1346 USA
800-521-0600

8c

THERMAL TRANSPIRATION IN THE SLIP FLOW REGIME

By

Lak-Tee Tang

A Thesis

Submitted to the Faculty of

Science and Engineering

of the University of Ottawa

in Partial Fulfillment of the

Requirements for the

Degree of

MASTER OF APPLIED SCIENCE

in Mechanical Engineering

September, 1970

ABSTRACT

The problem of thermal transpiration in the slip flow regime is studied from both theoretical and experimental aspects. Theoretical results are derived using boundary conditions obtained from kinetic theory considerations. Grad's method of solution of Boltzmann's equation is used to develop the slip velocity at the boundary. Consideration is also given here to surface interaction effects. Experiments have been carried out at Knudsen numbers from about 0.01 to 0.15. The theory is found to agree well with both the experimental data of Arney and Bailey and with the data reported here if σ, the fraction of molecules reflected diffusely, is assumed to be about 0.8. Theoretical pressure ratio vs. temperature ratio results are plotted in graphs with Knudsen number and σ as parameters.

THERMAL TRANSPIRATION IN THE SLIP FLOW REGIME

Advisor

Candidate

ACKNOWLEDGEMENTS

The author wishes to express his gratitude to his thesis advisor Dr. R.P. Henry, for his advice, guidance and encouragement throughout the course of this work. Funds were made available from the National Research Council of Canada, Grant No. 85568.

TABLE OF CONTENTS

LIST OF SYMBOLS

A	area
a	radius of a tube
c	thermal velocity
D_m	diameter of a molecule
d	diameter of a tube
f	distribution function
f_L	shifting factor
f_a	distribution function of molecules of type "a"
f_b	distribution function of molecules of type "b"
f_{dr}	distribution function of diffusely reflected molecules
f_i	distribution function of incident molecules
f_o	absolute Maxwellian distribution function
$f^{(\omega)}$	local Maxwellian distribution function
f_r	distribution function of reflected molecules
f_{sr}	distribution function of specularly reflected molecules
G	relative velocity
g	perturbation function
H	dimensionless thermal velocity
K_n	Knudsen number
K_{nc}	Knudsen number at the cold end of a tube
K_{nh}	Knudsen number at the hot end of a tube
k	Boltzmann's constant
k_1	a constant in Knudsen's semi-empirical formula, Eq. (2-3)
L	characteristic length
m	mass of a molecule
n	number of molecules per unit volume
p	pressure

P_h pressure at the hot end of a tube

P_{cl} pressure at the cold end of the large tube

P_{cs} pressure at the cold end of the small tube

P_r pressure ratio

P_{diff} pressure difference

Q defined quantity

R gas constant

R_m defined quantity

r cylindrical coordinate

s collision parameter

T temperature

T_c temperature at the cold end of a tube

T_h temperature at the hot end of a tube

T_i temperature of the incident molecules

T_r temperature ratio

T_{re} temperature of the reflected molecules

T_w temperature at the wall

t time

u_i component of macroscopic velocity in the i-direction, $i = 1,2,3$

u_z component of macroscopic velocity in the z-direction

X defined quantity

X_i component of force per unit mass in the i-direction, $i = 1,2,3$

x_i orthogonal coordinates, $i = 1,2,3$

y defined quantity

y_c defined quantity

y_h defined quantity

Z body force in the z-direction

z cylindrical coordinate or flow direction

α defined quantity

β defined quantity

ϵ reference angle on a plane perpendicular to the collision plane

ζ coefficient of slip

θ cylindrical coordinate

λ mean free path

μ viscocity

ν collision frequency

ξ_i component of absolute velocity in the i-direction, $i = 1,2,3$

σ fraction of molecules reflected diffusely

τ time between collisions

τ^* duration of a collision

ϕ_g defined quantity

χ elemental solid angle

ψ angle between relative velocity and line of impact

Note: Symbols with a bar overhead are average quantities

Primed symbols are quantities after collision

LIST OF FIGURES

LIST OF TABLES

1. INTRODUCTION

In pressure measurements at ordinary pressures, it is always assumed that the pressures at both ends of a tube are equal even when the temperatures at the ends are different. This is not true if the gas is at such a low pressure that the mean free path of the gas molecules becomes comparable with the diameter of the tube. Under these conditions, if the tube is unequally heated, there will be a resulting flow of gas along the tube even in the absence of a pressure gradient. If the circumstances are such as to prevent such a flow, for instance if one end of the tube is closed, then a steady pressure gradient may be set up with no net mass flow of the gas. This phenomena is known as thermal transpiration and, as indicated above, depends very strongly on the degree of rarefaction of the gas.

The parameter that indicates the degree of rarefaction of a gas is the Knudsen number K_n which is defined as the ratio of the mean free path λ to the characteristic dimension L of the body of interest. For the case of gas flow in a tube, the diameter of the tube is usually taken as the characteristic dimension. The mean free path is the average distance travelled by the gas molecules between collisions.

Gas dynamics can be roughly divided into the regions

of continuum flow, slip flow, transition flow and free-molecule flow. These are characterised by the degree of rarefaction as follows.

Continuum flow	$K_n < 0.01$
Slip flow	$0.01 < K_n < 0.1$
Transition flow	$0.1 < K_n < 10$
Free-molecule flow	$10 < K_n$

In the continuum flow regime, the properties of the flow are governed by the Navier-Stokes equations. In the last two regimes problems are solved by kinetic theory. In slip flow, where the Knudsen number is small but finite, greater difficulty is encountered. The Navier-Stokes equations can sometimes be used to solve problems provided that the boundary conditions are suitably modified.

In calibrating wind tunnel flows, one usually has to use pressure probes. In those cases where wind tunnel flows are used to simulate high speed aircraft or missile flight at high altitude, pressures interpreted by pressure probes may differ greatly from actual pressures as a result of thermal transpiration effects. Corrections have then to be made in order to give a true interpretation to pressure measured. To illustrate the importance of this effect, consider for example the limiting case of free-molecule flow. If the temperature at the hot end of a tube is four times that at the cold end, then the pressure at the hot end will be twice

that at the cold end (see Eq. 2-1). Therefore, if the pressure as sensed at the cold end is not corrected for the thermal transpiration effect, an error of 50% based on the true pressure is made.

2. LITERATURE SURVEY

The phenomena of thermal transpiration was first observed in the 1870's by Newmann and by Feddersen (1). They attributed it to the adsorption of gas in larger quantities at lower temperatures.

The problem was later treated by Maxwell and Knudsen using kinetic theory considerations (2,3). They were able to show that in the free-molecule flow regime, the temperature and pressure along a tube were related by

$$\frac{P}{\sqrt{T}} = \text{const.} \qquad 2\text{-}1$$

or expressed in differential form

$$\frac{dP}{P} = \frac{1}{2}\frac{dT}{T} \qquad 2\text{-}2$$

In the slip flow regime, Knudsen derived a semi-empirical formula (4)

$$\frac{dP}{dT} = \frac{1}{\frac{8}{3}\frac{1}{K_1}\frac{a}{\lambda} + \frac{\pi}{16}\frac{0.81}{0.49}\frac{a^2}{\lambda^2}\frac{1}{K_1}}\frac{P}{2T} \qquad 2\text{-}3$$

where K = 1 for small $\frac{a}{\lambda}$ and converges to a value between 2 to 3 for large $\frac{a}{\lambda}$.

Later, Knudsen published another relation derived

experimentally for the complete regime between continuum flow and free-molecule flow (3,4).

$$\frac{dp}{dT} = \frac{1}{\left[1 + 2.46\frac{a}{\lambda}\left(\frac{1 + 3.14\frac{a}{\lambda}}{1 + 24.6\frac{a}{\lambda}}\right)\right]^2} \cdot \frac{P}{2T} \qquad 2\text{-}4$$

Weber and Schmidt have also suggested a semi-empirical formula for Helium (5)

$$\log\left(\frac{P_h}{P_c}\right) = \frac{1}{2}\log\left(\frac{T_h}{T_c}\right) + 0.18131\log\left[(y_h + 0.1878)/(y_c + 0.1878)\right]$$
$$+ 0.41284\log\left[(y_h + 1.8311)/(y_c + 1.8311)\right] \qquad 2\text{-}5$$
$$- 0.15823\log\left[y_h + 4.9930)/(y_c + 4.9930)\right]$$

where $$y = \frac{a}{\lambda}$$

and λ satisfies $P\lambda = (P\lambda)_o (T/273.1)^{1+n}$.

$(P\lambda)_o$ is the value obtained at 0°C and n is obtained from

$$\frac{\mu}{\mu_o} = \left(\frac{T}{T_o}\right)^{\frac{1}{2}+n}$$

Liang(5), in an attempt to improve equation(2-5) derived a semi-empirical formula

$$\frac{P_h}{P_c} = \frac{\alpha_{He}(\phi_g X)^2 + \beta_{He}(\phi_g X) + R_m}{\alpha_{He}(\phi_g X)^2 + \beta_{He}(\phi_g X) + 1} \qquad 2\text{-}6$$

where $X = P_c d$, $R_m = \left(\frac{T_h}{T_c}\right)^{1/2}$, $\alpha_{He} = 2.52$

$$\beta_{He} = 7.68\left[1 - \left(\frac{T_h}{T_c}\right)^{1/2}\right]$$

To generalize equation (2-6) for other gases, Liang introduced a "shifting factor f_L" modifying equation (2-6) to

$$\frac{P_h}{P_c} = \frac{\alpha\left(\frac{X}{f_L}\right)^2 + \beta\left(\frac{X}{f_L}\right)^2 + R_m}{\alpha\left(\frac{X}{f_L}\right)^2 + \beta\left(\frac{X}{f_L}\right)^2 + 1} \qquad 2\text{-}7$$

where α and β are constants independent of the gas investigated and f_L is a function of the gas and temperature difference. Liang, using nitrogen, found the following values for α and β.

TABLE 2-1

Values of α and β at temperatures 195°K and 77.3°K

Temperature, K	α	β
195	22.76	5.00
77.3	29.5	12.5

With nitrogen as the standard and α and β given by Table 2-1, the shifting factor of several gases are (5):

TABLE 2-2

Values of shifting factors at temperatures 77.3°K and 195°K

Gas	Temperature °K	
	77.3	195
Nitrogen	1	1
Argon	1.25	1.3
Hydrogen	2.2	1.8
Helium	2.8	2.12

More recently, several workers attacked this problem experimentally. Such were Arney and Bailey (2,6) and Edmonds and Hobson (7). Arney and Bailey performed a series of experiments, using different gases and tubes of different sizes. Their experiments were by far the most intensive at that time and the results showed that Knudsen's semi-empirical formula adquately describes pressure variation with Knudsen number when the hot-to-cold temperature ratio is small (greater than but close to unity). They found that for Knudsen numbers greater than 2, the data for air began to exhibit an anomalous behavior. Instead of the values P_c/P_h tending towards the theoretical free molecule limit, applicable to the temperature ratio under consideration, there was a tendency for the ratio P_c/P_h to approach a minimum greater than the free-molecule value.

This ratio subsequently increases. Helium showed the same characteristics as air, but this phenomena occured only when the Knudsen number was greater than 10. They attributed this to the presence of a small pressure caused by outgassing. They further pointed out that Knudsen derived his semi-empirical formula from the experimental results of only one temperature ratio, 1.07. Hence they concluded that the deviation of experiment results from equation (2-4) might not be due to outgassing effects alone, but also due to temperature ratio as well.

Edmonds and Hobson (7) conducted a series of experiments in the free-molecule flow regime. Their results alsc show deviation from the theory of the free-molecule limit. They interpreted the failure of the limiting law for tubes as follows. A warm molecule has a greater probability of passing through a tube than a cold molecule. However, they were unable to give an analytical explanation, saying that such effect was evidently a complex one.

Kennard (8) attacked the problem in the slip flow regime by means of an analytical approach and gave

$$\frac{dp}{dT} = \frac{6\mu^2 R}{a^2 p\left(1 + \frac{4\zeta}{a}\right)} \qquad 2\text{-}8$$

where ζ is known as the coefficient of slip.

The following conclusions may be made from these previous studies:

The problem of thermal transpiration has been studied from both theoretical and experimental aspects. However, most of the existing theories are of semi-empirical nature except the one due to Kennard. Even this one was not obtained in a rigorous way. Kennard chose the boundary conditions to consist of two parts, one of which has no theoretical proof and was obtained by assuming that the velocity of slip is proportional to the velocity gradient, i.e. $\zeta \frac{du}{dz}$ Therefore it is hoped that in the light of new methods of solution of the Boltzmann equation developed in the past two decades, a deeper insight into the problem may be obtained. This is the main object of the present study.

3. THEORY

3-1 General Discussion

In the continuum regime, flow properties are governed by the Navier-Stokes equations along with a given set of boundary conditions. However, as the ratio of the mean free path of the gas molecule to the characteristic dimension of the system, i.e. the Knudsen number, becomes greater the Navier-Stokes equations will tend to be less accurate and will finally break down. Under these conditions one must resort to the use of Boltzmann's equation. This equation was first derived by James Clerk Maxwell in 1859 and was later put on a sounder basis by Ludwig Boltzmann (9). The full Boltzmann equation takes on the following form (10).

$$\frac{\partial f}{\partial t} + \xi_1 \frac{\partial f}{\partial x_1} + \xi_2 \frac{\partial f}{\partial x_2} + \xi_3 \frac{\partial f}{\partial x_3} + X_1 \frac{\partial f}{\partial \xi_1} + X_2 \frac{\partial f}{\partial \xi_2} + X_3 \frac{\partial f}{\partial \xi_3} = \left.\frac{df}{dt}\right|_{\text{collision}} \qquad 3\text{-}1$$

where in general $\left.\frac{df}{dt}\right|_{\text{collision}} = \iiint (f_a' f_b' - f_a f_b) G s \, ds \, d\epsilon \, d\xi_b$

and in particular, for smooth, rigid and elastic molecules,

$$\left.\frac{df}{dt}\right|_{\text{collision}} = \iint (f_a' f_b' - f_a f_b) D_m^2 G \cos\psi \, dx \, d\xi_2$$

3-1.1 Assumptions Involved in The Derivation of Boltzmann's Equation.

The Boltzmann equation is valid under the following assumptions:

(1) Molecular chaos prevails.

(2) Only binary collisions are considered. Collisions in which more than two molecules participate are assumed to be highly infrequent and their contribution in Boltzmann's equation is negligible.

(3) The time during which the molecules interact is assumed to be small compared with the time between collisions.

(4) The molecular dimensions are small compared with their mean free paths. This enable one to write f as a function of the variables ξ, x and t.

(5) The distribution function is only slowly varying. This assumption is equivalent to saying that f does not vary appreciably over a distance covered by the average molecule in the time dt, where

$$\tau^* \ll dt \ll \tau$$

and τ^* is the duration of a collision and τ is the time between collisions.

3-1.2 Application of The Boltzmann Equation.

The usual method of solving a problem would then

consist of the following steps:

(1) Solution of the Boltzmann equation to obtain the distribution function.

(2) With the distribution function known, the governing equation of the flow is obtained by substituting it into Maxwell's transfer equation (10):

$$\frac{\partial}{\partial t}(n\overline{Q}) + \frac{\partial}{\partial x_1}(n\overline{u_1 Q}) + \frac{\partial}{\partial x_2}(n\overline{u_2 Q}) + \frac{\partial}{\partial x_3}(n\overline{u_3 Q})$$

$$= \iiint (Q_a' - Q_b) f_a f_b G s \, d\epsilon \, ds \, d\xi_a \, d\xi_b \qquad 3\text{-}2$$

where $Q(u_1, u_2, u_3)$ is a quantity associated with each molecule, such as momentum (mu) or energy ($\frac{1}{2}mu^2$).

(3) The boundary conditions are found by evaluating appropriate moments of the distribution function. This is necessary because the boundary conditions differ greatly from those in continuum flow.

(4) With the governing equation and the boundary conditions obtained by the above procedure, the actual problem is then solved.

In the slip flow regime where the Knudsen number is small but finite, the Navier-Stokes equations still prove to be useful as the governing equations. Nevertheless, the boundary conditions still have to be modified with the knowledge of the distribution function.

3-1.3 General Methods of Solution of the Boltzmann Equation

Because of the nonlinear nature of the integro-differential Boltzmann Equation and because the range of phenomena encompassed by it is so great, no general method of obtaining an exact solution has so far been found. Instead, various approximate methods have been suggested. These methods fall into two major categories. One is to use an approximate method for solving the exact Boltzmann equation. The other involves modification of the Boltzmann equation itself. One technique based on the later method is due to Bhatnagar, Gross and Krook (11) proposed a relaxation model of the Boltzmann equation. In this method, the nonlinear collision integral term on the right hand side of equation (3-1) is replaced by

$$\nu(f_0 - f)$$

and the modified Boltzmann equation takes the form

$$\frac{\partial f}{\partial t} + \xi_j \frac{\partial f}{\partial x_j} + X_j \frac{\partial f}{\partial \xi_j} = \nu(f_0 - f)$$

This model simplifies the mathematics but retains many of the qualitative features of the true collision integral (12).

There are various techniques that fall into the first category. One of the simplest is to linearize the

Boltzmann equation. This is possible if the physical situation is such that f devaites only slightly from the absolute Maxwellian distribution, $f^{(0)}$. In this case, the distribution function can be represented by

$$f = f^{(0)}(1+\epsilon g)$$

Substitution of this f into the Boltzmann equation yields a simpler relation:

$$\frac{\partial g}{\partial t} + \xi_j \frac{\partial g}{\partial x_j} + X_i \frac{\partial g}{\partial \xi_i} = L(g)$$

where L(g) is a linear integral operator. This equation is simpler in that it is linear though it is still an integro-differential equation.

There is also another technique of solving the Boltzmann equation, which is known as the method of normal solution. This method was first proposed by Hilbert and later developed by Chapman and Enskog (13). It involves the expansion of the distribution function in terms of small parameters with $f^{(0)}$ as the first term in the expansion.

$$f = f^{(0)}\left[1 + \Phi_1 + \Phi_2 + \Phi_3 + \cdots\right]$$

Substituting this expansion into the Boltzmann

equation and equating like powers of the parameters yields a set of equations from which the functions ϕ_i in the expansion can be determined successively (12).

Grad (14) proposed the expansion of the distribution function in Hermite polynomials. He claimed that this method is suitable for flows with larger deviation from equilibrium (15). This method has been employed to obtain the distribution function in the present study. A brief description is provided in Appendix B.

3-1.4 Motion of Gas Molecules Near A Solid Boundary

In order to develop the boundary conditions for the present problem, it is necessary to know how the molecules interact with solid boundaries. The exact nature of the interaction of gas molecules with walls is very complicated.

When a gas molecule strikes a surface and is reflected at an angle equal to the angle of incidence, we say that the gas molecule is reflected specularly. There is no change of the tangential component of velocity. The normal component of velocity is reversed with no change in magnitude. If the distribution function of the incident molecules is Maxwellian, the reflected molecules will also have a Maxwellian distribution function. This is a result of the fact that it is a function of the square of the velocity. However, if the incident molecules have a non-Maxwellian distribution function, then

the distribution function of the incident molecules and that of the reflected molecules may be different but will be related by

$$f_r(\xi_1, \xi_2, \xi_3) = f_i(\xi_1, -\xi_2, \xi_3) \qquad 3\text{-}3$$

where f_r and f_i are the distribution functions of the reflected and incident molecules respectively. Equation (3-3) will be used later in the development of the boundary conditions.

On the other hand, a gas molecule on striking a surface, may sometimes be absorbed into the surface and thereby loose all its original momentum. Later it is released from the surface and flies off at an angle unrelated to the angle of incidence. This type of reflection is known as diffuse reflection. Whether or not the incident molecules have a Maxwellian distribution function, the reflected molecules will have a Maxwellian distribution function. These latter molecules are Maxwellian at a temperature which is in general not equal to the temperature of the incident gas or that of the wall. The relationship of these temperatures will be discussed later.

Experiments have shown that when gas molecules strike a solid boundary, they are not all reflected either specularly or diffusely (16). Instead, some fraction are reflected specularly while others are reflected diffusely. The figure

below shows the typical nature of reflection. The length of the arrow indicates the probability of the molecule being reflected in that direction. θ_i is the angle of incidence.

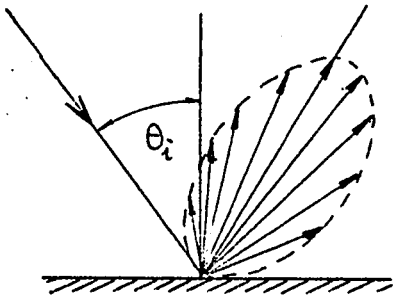

For convenience of analysis, it is always neccessary to define a constant σ as the fraction of molecules reflected diffusely and $(1-\sigma)$ as the fraction of molecules reflected specularly. The value of σ depends on the type of gas and the type of surface and may even depend on the temperatures of the gas and of the surface. (16)

3-1.5 Coefficient of Thermal Accommodation

As stated in section 3-1.4, it is sometimes noted that the temperature of the reflected molecules is not always equal to that of the solid boundary or that of the incident gas. For this Knudsen (3) introduced what he called a coefficient of thermal accommodation as follows:

$$\alpha = \frac{T_{re} - T_i}{T_w - T_i} \qquad 3\text{-}4$$

This expression relates the temperature of the incident molecules T_i , of the wall T_w and of the reflected molecules T_{re}.

3-2 Thermal Transpiration in The Slip Flow Regime

To develop the boundary conditions, consider an elemental area ΔA in the region of the boundary.

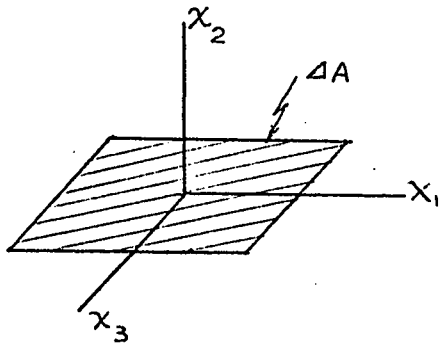

By definition of the distribution function, $f d\xi_1 d\xi_2 d\xi_3$ represents the number of molecules per unit volume and having velocities lying between ξ and $(\xi + d\xi)$.

The number of molecules with velocities between ξ and $(\xi + d\xi)$ striking an elemental area ΔA per unit time will be

$$\vec{\xi} \cdot \vec{n} \Delta A f d\xi_1 d\xi_2 d\xi_3$$

$$= \xi_2 \Delta A f d\xi_1 d\xi_2 d\xi_3$$

where $\vec{n}$ is the unit normal vector of the elemental area ΔA.

The total number of molecules striking ΔA per unit time will be

$$\int_{-\infty}^{\infty}\int_{-\infty}^{\infty}\int_{-\infty}^{\infty} \xi_2 \Delta A f d\xi_1 d\xi_2 d\xi_3$$

Over unit area, this is

$$\int_{-\infty}^{\infty}\int_{-\infty}^{\infty}\int_{-\infty}^{\infty} \xi_2 f \, d\xi_1 d\xi_2 d\xi_3$$

Therefore the tangential component of momentum flux in the x_1-direction is

$$m \int_{-\infty}^{\infty}\int_{-\infty}^{\infty}\int_{-\infty}^{\infty} \xi_1 \xi_2 f \, d\xi_1 d\xi_2 d\xi_3$$

This is made up of the momentum flux in the x_1- direction associated with the incident molecules, the diffusely reflected molecules and the specularly reflected molecules. Thus,

$$m \int_{-\infty}^{\infty}\int_{-\infty}^{\infty}\int_{-\infty}^{\infty} \xi_1 \xi_2 f \, d\xi_1 d\xi_2 d\xi_3$$

$$= m \int_{-\infty}^{\infty}\int_{-\infty}^{0}\int_{-\infty}^{\infty} \xi_1 \xi_2 f \, d\xi_1 d\xi_2 d\xi_3 + \sigma m \int_{-\infty}^{\infty}\int_{0}^{\infty}\int_{-\infty}^{\infty} \xi_1 \xi_2 f_{dr} \, d\xi_1 d\xi_2 d\xi_3 \qquad 3\text{-}5$$

$$+ (1-\sigma) m \int_{-\infty}^{\infty}\int_{c}^{\infty}\int_{-\infty}^{\infty} \xi_1 \xi_2 f_{sr} \, d\xi_1 d\xi_2 d\xi_3$$

It is convenient to represent equation (3-5) by $I_L = I_{R1} + I_{R2} + I_{R3}$

Note that:

(1) $\xi_1 = u_1 + c_1$

(2) $\xi_2 = u_2 + c_2 = c_2$ since the normal component of the macroscopic velocity at the boundary is zero.

(3) f is given by equation (B-1), Appendix B

(4) $f_{sr}(\xi_1, \xi_2, \xi_3) = f_i(\xi_1, -\xi_2, \xi_3)$

(5) $f_{dr} = f_o$ corresponding to the temperature T_{re} given by Eq.(3-4).

(6) $RT = \frac{1}{3}\overline{c^2}$ (Ref. 10)

(7) $d\xi_i = dc_i$

Substituting these quantities into equation (3-5) and expanding in terms of the Hermite Polynomials, retaining the first three terms , yields

$$I_L = \int_{-\infty}^{\infty}\int_{-\infty}^{\infty}\int_{-\infty}^{\infty}(u_1+\sqrt{RT}H_1)\sqrt{RT}H_2\cap(2\pi RT)^{-3/2}e^{-\frac{1}{2}H^2}\Big[1+a_1H_1+a_2H_2+a_3H_3+\tfrac{1}{2}a_{11}H_1^2$$

$$+\tfrac{1}{2}a_{12}H_1H_2+\tfrac{1}{2}a_{13}H_1H_3+\tfrac{1}{2}a_{21}H_2H_1+\tfrac{1}{2}a_{22}H_2H_2$$

$$+\tfrac{1}{2}a_{23}H_2H_3+\tfrac{1}{2}a_{31}H_3H_1+\tfrac{1}{2}a_{32}H_3H_2+\tfrac{1}{2}a_{33}H_3H_3$$

$$+\tfrac{1}{6}\Big(a_{111}H_1H_1H_1+a_{112}H_1H_1H_2+a_{113}H_1H_1H_3$$

$$+a_{121}H_1H_2H_1+a_{122}H_1H_2H_2+a_{123}H_1H_2H_3$$

$$+a_{131}H_1H_3H_1+a_{132}H_1H_3H_2+a_{133}H_1H_3H_3$$

$$+a_{211}H_2H_1H_1+a_{212}H_2H_1H_2+a_{213}H_2H_1H_3$$

$$+a_{221}H_2H_2H_1+a_{222}H_2H_2H_2+a_{223}H_2H_2H_3$$

$$+a_{231}H_2H_3H_1 \quad + a_{232}H_2H_3H_2 + a_{233}H_2H_3H_3$$

$$+a_{311}H_3H_1H_1 + a_{312}H_3H_1H_2 + a_{313}H_3H_1H_3$$

$$+a_{321}H_3H_2H_1 + a_{322}H_3H_2H_2 + a_{323}H_3H_2H_3$$

$$+a_{331}H_3H_3H_1 + a_{332}H_3H_3H_2 + a_{333}H_3H_3H_3\Big)\cdot$$

$$\cdot\left[\sqrt{RT}\,dH_1\sqrt{RT}\,dH_2\sqrt{RT}\,dH_3\right]$$

$$I_{R1} = \int_{-\infty}^{\infty}\int_{-\infty}^{0}\int_{-\infty}^{\infty}(u_1+\sqrt{RT}H_1)\sqrt{RT}H_2\,n(2\pi RT)^{-3/2}e^{-\frac{1}{2}H^2}\Big[1+a_1H_1+a_2H_2+a_3H_3$$

$$+\tfrac{1}{2}\big(a_{11}H_1H_1+ a_{12}H_1H_2 + a_{13}H_1H_3 + a_{21}H_2H_1$$

$$+a_{22}H_2H_2 + a_{23}H_2H_3 + a_{31}H_3H_1 + a_{32}H_3H_2 + a_{33}H_3H_3\big)$$

$$+\tfrac{1}{6}\big(a_{111}H_1^3 + a_{112}H_1H_1H_2 + a_{113}H_1H_1H_3$$

$$+a_{121}H_1H_2H_1 + a_{122}H_1H_2H_2 + a_{123}H_1H_2H_3$$

$$+a_{131}H_1H_3H_1 + a_{132}H_1H_3H_2 + a_{133}H_1H_3H_3$$

$$+a_{211}H_2H_1H_1 + a_{212}H_2H_1H_2 + a_{213}H_2H_1H_3$$

$$+a_{221}H_2H_2H_1 + a_{222}H_2H_2H_2 + a_{223}H_2H_2H_3$$

$$+a_{231}H_2H_3H_1 + a_{232}H_2H_3H_2 + a_{233}H_2H_3H_3$$

$$+a_{311}H_3H_1H_1 + a_{312}H_3H_1H_2 + a_{313}H_3H_1H_3$$

$$+a_{321}H_3H_2H_1 + a_{322}H_3H_2H_2 + a_{323}H_3H_2H_3$$

$$+a_{331}H_3H_3H_1 + a_{332}H_3H_3H_2 + a_{333}H_3H_3H_3)\Big] \cdot$$

$$\cdot\left[\sqrt{RT}\, dH_1 \sqrt{RT}\, dH_2 \sqrt{RT}\, dH_3\right]$$

$$I_{R2} = \sigma \int_{-\infty}^{\infty}\int_{0}^{\infty}\int_{-\infty}^{\infty} (\sqrt{RT}\,H_1)(\sqrt{RT}\,H_2)\, n (2\pi RT_r)^{-3/2} e^{-\frac{1}{2}H^2} (RT)^{3/2} dH_1 dH_2 dH_3$$

$$I_{R3} = (1-\sigma)\int_{-\infty}^{\infty}\int_{0}^{\infty}\int_{-\infty}^{\infty} (u_1 + \sqrt{RT}\,H_1)(-\sqrt{RT}\,H_2)\, n (2\pi RT)^{-\frac{3}{2}} e^{-\frac{1}{2}H^2} \cdot$$

$$\cdot\Big[1 + a_1H_1 - a_2H_2 + a_3H_3 + \tfrac{1}{2}\left(a_{11}H_1^2 - a_{12}H_1H_2 + a_{13}H_1H_3\right.$$

$$\left. - a_{21}H_2H_1 + a_{22}H_2H_2 - a_{23}H_2H_3 + a_{31}H_3H_1 - a_{32}H_3H_2 + a_{33}H_3^2\right)$$

$$+\frac{1}{6}\left(a_{111}H_1^3 - a_{112}H_1H_1H_2 + a_{113}H_1H_1H_3\right.$$

$$- a_{121}H_1H_2H_1 + a_{122}H_1H_2H_2 - a_{123}H_1H_2H_3$$

$$+ a_{131}H_1H_3H_1 - a_{132}H_1H_3H_2 + a_{133}H_1H_3H_3$$

$$- a_{211}H_2H_1H_1 + a_{212}H_2H_1H_2 - a_{213}H_2H_1H_3$$

$$+ a_{221}H_2H_2H_1 - a_{222}H_2H_2H_2 + a_{223}H_2H_2H_3$$

$$- a_{231}H_2H_3H_1 + a_{232}H_2H_3H_2 - a_{233}H_2H_3H_3$$

$$+ a_{311}H_2H_3H_2 - a_{312}H_3H_1H_2 + a_{313}H_3H_1H_3$$

$$- a_{321}H_3H_2H_1 + a_{322}H_3H_2H_2 - a_{323}H_3H_2H_3$$

$$\left. + a_{331}H_3H_3H_1 - a_{332}H_3H_3H_2 + a_{333}H_3^3\right)\Big]\cdot$$

$$\cdot\left[\sqrt{RT}\,dH_1\sqrt{RT}\,dH_2\sqrt{RT}\,dH_3\right]$$

Integrate the above equations with the help of the integral formulae in Appendix A. Note that the order of the subscript numbers in a_{ij} and a_{ijk} is immaterial.

$$\sqrt{RT}\,u_1\left[a_2+\tfrac{1}{2}a_{112}+\tfrac{1}{2}a_{222}+\tfrac{1}{2}a_{233}\right]+RT\,a_{12}$$

$$=\sqrt{RT}\left[(2\pi)^{-1/2}u_1+\tfrac{1}{2}a_2+\tfrac{1}{4}a_{112}+\tfrac{1}{4}a_{222}+\tfrac{1}{4}a_{233}\right]$$

$$-(2\pi)^{-\frac{1}{2}}RT\left[a_1+\tfrac{1}{2}a_{111}+\tfrac{1}{2}a_{122}+\tfrac{1}{2}a_{133}\right]-(2\pi)^{-\frac{1}{2}}RT\cdot\tfrac{1}{2}a_{122}$$

$$-(2\pi)^{-\frac{1}{2}}(RT)^{1/2}u_1\left[\tfrac{1}{2}a_{11}+\tfrac{1}{2}a_{22}+\tfrac{1}{2}a_{33}\right]-\tfrac{1}{2}(2\pi)^{-1/2}\sqrt{RT}\,u_1\,a_{22}$$

$$-\tfrac{1}{2}RT\,a_{12}+(1-\sigma)RT(2\pi)^{-1/2}\left[a_1+\tfrac{1}{2}a_{111}+\tfrac{1}{2}a_{122}+\tfrac{1}{2}a_{133}+\tfrac{1}{2}a_{122}\right]$$

$$-(1-\sigma)(RT)^{1/2}u_1\left[\tfrac{1}{2}a_2+\tfrac{1}{4}a_{112}+\tfrac{1}{4}a_{222}+\tfrac{1}{4}a_{233}\right]$$

$$+(1-\sigma)(RT)^{1/2}(2\pi)^{-1/2}u_1\left[\tfrac{1}{2}a_{11}+\tfrac{1}{2}a_{22}+\tfrac{1}{2}a_{33}+\tfrac{1}{2}a_{22}\right]$$

$$-(1-\sigma)RT\cdot\tfrac{1}{2}a_{12}+(1-\sigma)(2\pi)^{-\frac{1}{2}}(RT)^{1/2}u_1$$

The above equation can be further simplied using the relations (B-2) and (B-3):

$$2a_i + a_{ijj} = 0$$

$$a_{ii} = 0$$

Thus

$$RT a_{12} = -(2\pi)^{-1/2}(RT)^{1/2} u_1 - \tfrac{1}{2}(2\pi)^{-1/2} RT\, a_{122} + \tfrac{1}{2} RT\, a_{12}$$

$$-\tfrac{1}{2}(2\pi)^{-1/2}(RT)^{1/2} u_1 a_{22} - \tfrac{1}{2}(1-\sigma)(2\pi)^{-1/2} RT\, a_{122}$$

$$+\tfrac{1}{2}(1-\sigma)(2\pi)^{-1/2}(RT)^{1/2} u_1 a_{22} - \tfrac{1}{2}(1-\sigma) RT\, a_{12}$$

$$+(1-\sigma)(2\pi)^{-1/2}(RT)^{1/2} u_1$$

Finally,

$$u_1 = \sqrt{RT}\left[\tfrac{1}{2} a_{122} + \frac{2-\sigma}{\sigma}\sqrt{\frac{\pi}{2}}\, a_{12}\right] \Big/ \left[\tfrac{1}{2} a_{22} - 1\right] \qquad 3\text{-}6$$

Patterson's results (10) are used for the coefficients of the Hermite Polynomials. For one dimensional flow in the x_1-direction, $u_2 = u_3 = 0$. Thus from equations (B-4) to (B-6),

$$a_{12} = -\frac{\mu}{mnRT}\frac{\partial u_1}{\partial x_2}$$

$$a_{zz} = \frac{2}{3} \frac{\mu}{mnRT} \frac{\partial u_1}{\partial x_1}$$

$$a_{1zz} = -\frac{3}{2} \frac{\mu}{mn} (RT)^{-\frac{3}{2}} R \frac{\partial T}{\partial x_1}$$

where $\overline{c^2} = 3RT$ has been used.

Substituting these coefficients into equation (3-6) yields,

$$u_1 = \frac{\left[\frac{3}{4} \frac{\mu}{mn} \frac{1}{T} \frac{\partial T}{\partial x_1} + \frac{2-\sigma}{\sigma} \frac{\mu}{mn} \sqrt{\frac{\pi}{2RT}} \frac{\partial u_1}{\partial x_2}\right]}{\left[1 - \frac{1}{3} \frac{\mu}{mnRT} \frac{\partial u_1}{\partial x_1}\right]} \qquad 3\text{-}7$$

Equation (3-7) gives the slip velocity at the boundary for one-dimensional flow in the x_1 direction. With the slip velocity given by the above equation, it is now possible to find an expression for the velocity distribution. This will be done in the next section.

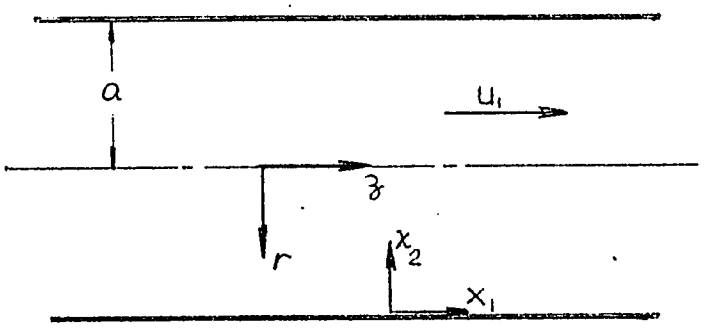

Consider now the flow of gas in a tube with radius "a" as shown in the above figure.

As atated in section 3-1.2, the Navier-Stokes equations are valid for the slip flow regime provided the boundary conditions are suitably modified.

The complete Navier-Stokes equation of motion in the axial direction in cylindrical coordinates is (17)

$$\rho \frac{DU_z}{Dt} = Z - \frac{\partial P}{\partial z} + \frac{\partial}{\partial z}\left[\mu\left(2\frac{\partial u_z}{\partial z} - \frac{2}{3}\nabla\cdot\vec{U}\right)\right]$$

$$+ \frac{1}{r}\frac{\partial}{\partial r}\left[\mu r\left(\frac{\partial u_z}{\partial z} + \frac{\partial u_z}{\partial r}\right)\right] + \frac{1}{r}\frac{\partial}{\partial \theta}\left[\mu\left(\frac{1}{r}\frac{\partial u_z}{\partial \theta} + \frac{\partial u_\theta}{\partial z}\right)\right]$$

where $$\frac{D}{Dt} = \frac{\partial}{\partial t} + u_r\frac{\partial}{\partial r} + \frac{u_\theta}{r}\frac{\partial}{\partial \theta} + u_z\frac{\partial}{\partial z} \qquad 3\text{-}8$$

and $$\nabla\cdot\vec{U} = \frac{1}{r}\frac{\partial(r u_r)}{\partial r} + \frac{1}{r}\frac{\partial u_\theta}{\partial \theta} + \frac{\partial u_z}{\partial z}$$

The continuity equation is (17)

$$\frac{\partial \rho}{\partial t} + \frac{1}{r}\frac{\partial(\rho u_r r)}{\partial r} + \frac{1}{r}\frac{\partial(\rho u_\theta)}{\partial \theta} + \frac{\partial(\rho u_z)}{\partial z} = 0 \qquad 3\text{-}9$$

For the present problem, the following assumptions are made:

(a) Steady incompressible fluid flow.

(b) Body force is negligible, Z=0.

(c) No applied force in the axial direction, i.e. no acceleration term in this direction, $\frac{Du_z}{Dt}=0$

(d) Flow is symmetrical about z-axis, $\frac{\partial}{\partial\theta}=0$

(e) One-dimensional flow, $u_z \neq 0$, $u_\theta = u_r = 0$

From the continuity equation and assumptions (a) and (e),

$$\frac{\partial u_z}{\partial z} = 0 \qquad 3\text{-}10$$

Using the above assumptions and equation (3-10), the Navier-Stokes equation (3-8) is reduced to

$$\mu \frac{d^2u_z}{dr^2} + \frac{\mu}{r}\frac{du_z}{dr} = \frac{dp}{dz} \qquad 3\text{-}11$$

Integrating equation (3-11) with respect to r yields

$$\frac{du_z}{dr} = \frac{r}{2\mu}\frac{dp}{dz} + \frac{c_1}{r}$$

where c_1 is an integration constant.

By symmetry, $\frac{du_z}{dr} = 0$ at r=0

Thus $c_1 = 0$ and

$$\frac{du_z}{dr} = \frac{r}{2\mu}\frac{dp}{dz} \qquad 3\text{-}12$$

Integrating again with respect to r

$$u_z = \frac{r^2}{4\mu}\frac{dp}{dz} + c \qquad 3\text{-}13$$

where c is another integration constant.

Here it is necessary to determine c from the boundary condition (3-7).

Replacing

$$u_1 \text{ by } u_z, \quad \frac{\partial}{\partial x_1} \text{ by } \frac{\partial}{\partial z} \text{ and } \quad \frac{\partial}{\partial x_2} \text{ by } \left(-\frac{\partial}{\partial r}\right)$$

and using equations (3-10) and (3-12) with r=a, equation (3-7) becomes

$$u_z\Big]_{r=a} = \left[\frac{3}{4}\frac{\mu}{mn}\frac{1}{T}\frac{dT}{dz} - \frac{2-\sigma}{\sigma}\frac{a}{2mn}\sqrt{\frac{\pi}{2RT}}\frac{dp}{dz}\right]_{\text{at } r=a} \qquad 3\text{-}14$$

Obtaining c from equations (3-13) and (3-14) and substituting it into equation (3-13) yields

$$u = \left[\frac{r^2}{4\mu} - \frac{a^2}{4\mu} - \frac{2-\sigma}{\sigma}\frac{a}{2mn}\sqrt{\frac{\pi}{2RT}}\right]\frac{dp}{dz} + \frac{3}{4}\frac{\mu}{mn}\frac{1}{T}\frac{dT}{dz} \qquad 3\text{-}15$$

which is the velocity distribution across the section perpendicular to the direction of flow.

With the velocity distribution given by equation (3-15), it is now possible to find an expression for the mass flow rate across any section perpendicular to the direction of flow.

$$\dot{Q}_m = \int_A mn u \, dA$$

$$= \int_0^a mn \left[\left(\frac{r^2}{4\mu} - \frac{a^2}{4\mu} - \frac{2-\sigma}{\sigma} \frac{a}{2mn} \sqrt{\frac{\pi}{2RT}} \right) \frac{dP}{dz} + \frac{3}{4} \frac{\mu}{mn} \frac{1}{T} \frac{dT}{dz} \right] 2\pi r \, dr$$

$$= \pi mn \left[\left(\frac{a^4}{8\mu} - \frac{a^4}{4\mu} - \frac{2-\sigma}{\sigma} \frac{a^3}{2mn} \sqrt{\frac{\pi}{2RT}} \right) \frac{dP}{dz} + \frac{3}{4} \frac{\mu a^2}{mn} \frac{1}{T} \frac{dT}{dz} \right]$$

For the problem of thermal transpiration, the equilibrium state is reached when there is no net mass flow across any section perpendicular to the axis of the tube. Thus

$$\dot{Q}_m = 0$$

$$\frac{dP}{dT} = \frac{\frac{3}{4} \frac{\mu}{mn} \frac{1}{T}}{\frac{a^2}{8\mu} + \frac{2-\sigma}{\sigma} \cdot \frac{a}{2mn} \sqrt{\frac{\pi}{2RT}}} \qquad 3\text{-}16$$

This is the equation that governs the change of pressure with respect to the change of temperature of gas flow along a small tubing in the slip flow regime. For practical purposes, it will be more convenient if the above equation is expressed in terms of dimensionless parameters.

Note that $m_n = \rho$

and $P = \rho RT$ for a perfect gas.

Using the relation for mean free path (10)

$$\lambda = \frac{16}{5} \frac{\mu}{\rho \sqrt{2\pi RT}}$$

equation (3-16) becomes

$$\frac{\frac{dP}{P}}{\frac{dT}{T}} = \frac{\frac{3}{2} K_n}{\frac{4}{5} \frac{2-\sigma}{\sigma} + \frac{8}{25\pi} \frac{1}{K_n}} \qquad 3\text{-}17$$

where the Knudsen number K_n is defined as the ratio of the mean free path to the diameter of the tube in which the gas flows.

$$K_n = \frac{\lambda}{d}$$

Using the expressions for mean free path and viscosity (10)

$$\lambda = \frac{16}{5} \frac{\mu}{\rho \sqrt{2\pi RT}}$$

$$\mu = \frac{5m}{16\pi^{1/2} D_m^2} \left(\frac{\overline{c^2}}{3} \right)^{1/2} = \frac{5m}{16\sqrt{\pi} D_m^2} \sqrt{RT}$$

and $$K_n = \frac{\lambda}{d} = \frac{mR}{\pi\sqrt{2} D^2 d} \frac{T}{P} = \text{constant} \times \frac{T}{P}$$

then $$\frac{dK_n}{K_n} = \frac{dT}{T} - \frac{dP}{P} \qquad 3\text{-}18$$

Equations (3-17) and (3-18) yield

$$\frac{dT}{T} = \frac{\frac{4}{5} \frac{2-\sigma}{\sigma} K_n + \frac{8}{25\pi}}{K_n \left[-\frac{3}{2} K_n^2 + \frac{4}{5} \frac{2-\sigma}{\sigma} K_n + \frac{8}{25\pi} \right]} dK_n \qquad 3\text{-}19$$

Equations (3-18) and (3-19) are integrated to give the following expressions (Appendix C)

$$\frac{K_{nh}}{K_{nc}} = \frac{T_h}{T_c} \cdot \frac{P_c}{P_h} \qquad 3\text{-}20$$

and

$$\frac{T_h}{T_c} = \frac{K_{nh}}{K_{nc}} \left[\frac{A K_{nh}^2 + B K_{nh} + C}{A K_{nc}^2 + B K_{nc} + C} \right]^{-\frac{1}{2}} \left[\frac{(2AK_{nh}+B-D)(2AK_{nc}+B+D)}{(2AK_{nh}+B+D)(2AK_{nc}+B-D)} \right]^{\frac{B}{2D}} \quad 3\text{-}21$$

where $A = -\frac{3}{2}$, $B = \frac{4}{5}\frac{2-\sigma}{\sigma}$, $C = \frac{8}{25\pi}$

and $D = \sqrt{B^2 - 4AC}$

Equations (3-20) and (3-21) give the relationship between the temperature ratio and the pressure ratio, with K_{nc} (or K_{nh}) and σ as the determining parameters. For a given set of values of $\frac{T_h}{T_c}$ and K_{nc}, K_{nh} is determined by equation (3-21). $\frac{P_h}{P_c}$ is then obtained from equation (3-20).

For practical purposes, graphs of $\frac{P_c}{P_h}$ vs $\frac{T_h}{T_c}$ are plotted for different values of K_{nc} and σ and shown in figures (9) to (12).

4. EXPERIMENTS

4-1 Design of the System

The design of the whole system was chosen so that it was simple, inexpensive and yet effective over a wide vacuum range. For this reason, the number of valves and couplings was reduced to as few as possible. Where welding or soldering was feasible, a coupling was avoided. Though this procedure had the defect that later rearrangement of the system was made more difficult, it had the most important advantage that the possibility of vacuum leaks was reduced.

Figure (4-1) shows the arrangement of the apparatus for this experiment. Basically, it consists of a small tube t_S enclosed in a larger tube t_L , the latter with two removable end plates. A heater H and a cooling coil CC are mounted, one on each end of the small tube. The cold end of the small tube is connected to one of the sensing ports of the differential pressure transducer. The other sensing port is in turn connected to the cold end of the large tube at point C_L.

In order that the small tubing may be changed, a coupling was employed for this purpose at the point C_S. The

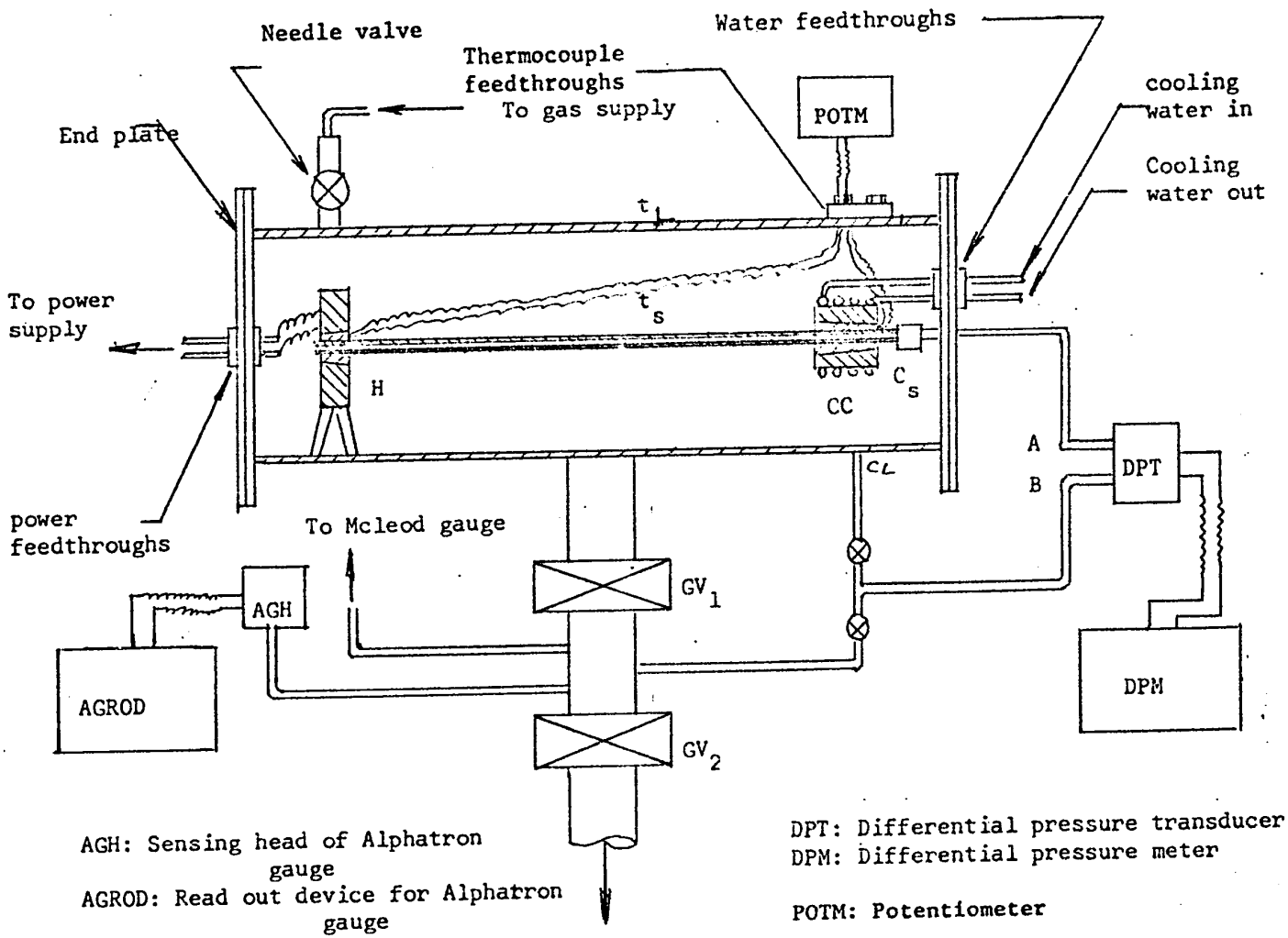

Figure (4-1) A Schematic Diagram of the Experimental Apparatus

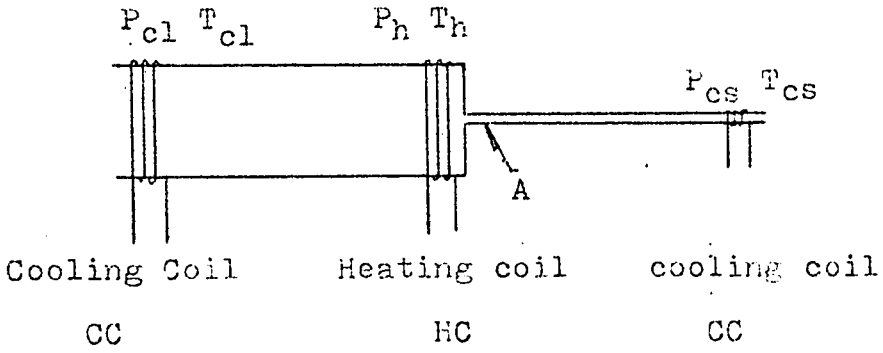

Figure (4-2) Arrangement of large and small tubes (1)

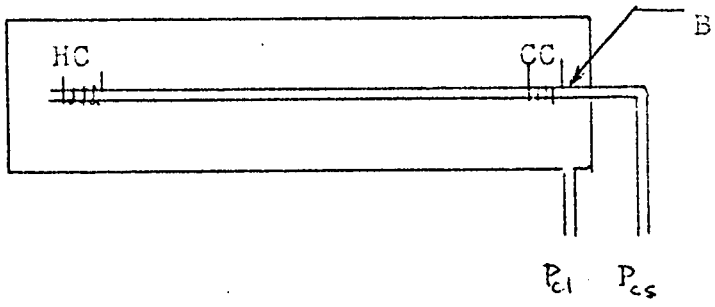

Figure (4-3) Arrangement of large and small tubes (2)

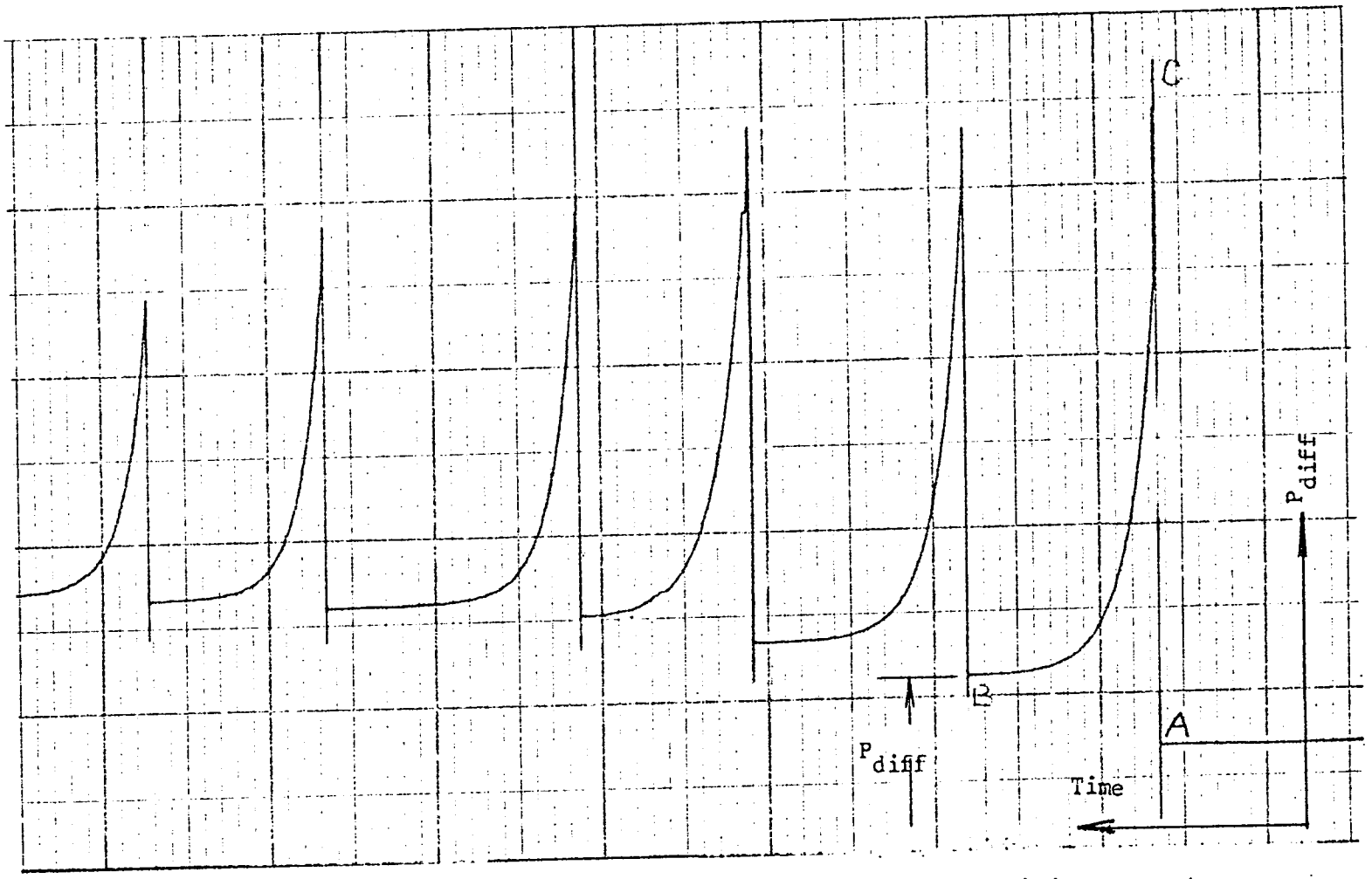

At point A, gas is bled in and the pressure difference $(P_{cl}-P_{cs})$ increases to a value corresponding to point C. The needle valve is then closed and the pressure difference desreases to a value corresponding to point B. This value is taken as that due to thermal transpiration.

Figure (4-4) Recorded Trace of Variation of Pressure Difference With Time

gas to be tested is bled in through the needle valve situated on top of the large tube t_L. On one of the end plates, power feed-throughs are mounted to supply electric current to the heater inside the vessel. Cooling water is supplied to the cooling coil by means of water feed-throughs situated in the other end plate. The whole system is connected to a NRC model HS-2-300 diffusion pump DP and a Welch model 1402B mechanical pump MP. Between the main vessel and the pumps is a small manifold reference section separated by means of two gate valves GV_1 and GV_2. A Mcleod gauge and an Alphatron ionization gauge are connected to the reference vacuum section.

In the experiment, it was necessary to measure the pressure difference between the hot end and the cold end of the small tubing and also the absolute pressure at the cold end; all corresponding to a given temperature ratio at the ends of the tube. Since most vacuum gauges are designed to measure pressures of gases at or close to room temperature, the difference in pressures at the hot and cold ends could not be measured by directly connecting the sensing ports of a pressure transducer to the two ends of the small tubing under test. For this reason, a relative method was employed. In this, the small tubing was connected to a much larger tube as shown in Figure (4-2). Instead of measuring the pressure difference between the ends of the small tubing, i.e. $P_h - P_c$, the pressure difference ($P_{c1} - P_{c2}$) was measured. The diameter

of the larger tube was chosen to be large enough so that the Kundsen number was very small. In this way the thermal transpiration effect occuring in it could be neglected and the difference ($P_{c1} - P_{c2}$) could be taken as the required value ($P_h - P_{c2}$). If the Knudsen number in the large tube, hoever, were too great, then the difference between P_{c1} and P_h would have to be taken into account and added to ($P_{c1} - P_{c2}$) to give the required value of ($P_h - P_{c2}$).

Instead of choosing about one inch diameter for the large tube as done by other experimenters (2,6), a pipe of six inches diameter was selected. Small tubing of 0.03 inch diameter would have allowed the performing of experiments up to a Knudsen number of 2 while the large tube retained a Knudsen number less than 0.01. At this large tube Knudsen number, the effect of thermal transpiration is so small that the difference in pressures at the ends of the tube can be neglected. Thus it would have been possible to conduct experiments up to a Knudsen number of 2 in the small tube without the necessity of correcting for differences between P_h and P_{c1} .

The arrangement of the small and large tubes for the present experiment is shown in Figure (4-3). This has the following advantages over that shown in Figure (4-2):

(1) In order that the small tubing may be changed if necessary, a vacuum coupling at the point A of Figure (4-2) or point

B in Figure (4-3) is necessary. Unless the whole assembly of Figure (4-2) is installed in a large vacuum chamber (as Arney and Bailey did in their experiments), a coupling at that point can cause great errors due to small leakage of air. Also, since point A in Figure (4-2) is close to the heated end, it is doubtful if the O-ring inside the coupling would be able to withstand the temperatures resulting from heating by conduction through the tube from the heater.

(2) With the arrangement shown in Figure (4-3), it is possible to mount the heater on the small tubing. In this way, the difference in temperatures at the ends of the tube is greatly reduced. This will have a further effect in reducing the pressure difference between the hot and cold ends of the large tube, ($P_h - P_{cl}$).

4-2 Instrumentation

For the experiment it was necessary to measure the pressure difference ($P_h - P_{cs}$), the absolute pressure at the cold end of the small tube and the temperatures at the ends of the tube.

The pressure difference ($P_{cl} - P_{cs}$) is measured by means of a MKS Type 77H differential pressure transducer together with a MKS Baratron Type 77 Electronic Pressure Meter for read out. This particular type of pressure transducer has

the capability of measuring pressure differences in the range from 3×10^{-4} torr to 1 torr, with a maximum resolution power of 1×10^{-5} torr (which is equivalant to 1/76,000,000 of an atmospheric pressure). The pressure difference resolution sought for the experiments was of the order of 10^{-3} torr (or one micron mercury).

The absolute pressure is measured by means of an Alphatron Type 8200 ionization gauge from Norton Company. This Alphatron ionization gauge is capable of measuring pressures from 1000 torr to 10^{-4} torr with a greatest resolution power of 1×10^{-5} torr. Using small tubing of 0.03 inch in diameter, this gauge is capable of covering the whole range from continuum through slip flow to free-molecule flow.

Temperatures are measured by means of K-type thermocouples (chromel-alumel) embeded at both ends of the tube. A Leeds and Northrup potentiometer is used to measure the thermocouple outputs.

Pressures and temperatures are monitored on a Hewlett Packard 7100B strip chart recorder to check for establishment of steady state conditions.

4-3 Preliminary Tests

Some preliminary tests were carried out prior to taking data. Initially small leaks caused a great deal of trouble,

however, using the Alphatron pressure gauge as a leak detector, most were found and corrected. When the gate valve GV1 was closed after the system had been pumped for about 24 hours, the rate of increase of pressure was found to be about 25 microns mercury per hour. Further attempts to reduce this rate were not fruitful. It was suspected that most of the remaining problem was likely due to outgassing effects possibly along with a combination of small leaks through the joints.

Tests to establish length of time to reach equilibrium were conducted. The results showed that there was always a pressure difference between the two points A and B (Fig. 4-1), with P_A greater than P_B . This occured both with and without the heater on. It is believed that this is a result of the low conductance of the small tubing. That is, at very low pressures, it takes a very long time for the portion of gas in the line $C_s A$ to reach the same pressure as the gas in the chamber.

Precautions were taken to check that the temperature at the cold end of the large tube was at or close to room temperature. Since there is no cooling coil in contact with this end, the temperature is maintained by natural convection. Measurement of temperature at that end showed that under no conditions did it reach more than 100°F.

4-4 Experimental Procedure

The chamber was first evacuated to as low a pressure as possible ($\sim 10^{-3}$ torr), then the test gas was introduced through the needle valve and the pressure raised to about one-half atmosphere. This procedure was repeated several times to ensure that the initial air had been completely flushed from the system. The heater was switched on at the beginning of the experiment in order to assist outgassing.

After the final filling with test gas, the system was continuously pumped with the heater on for about twenty-four hours in order to permit outgassing and reaching as low a steady state pressure as possible.

By this time the temperatures at both ends of the small tube had reached a steady state. Next, the gate valve GV_1 was closed and a little gas was bled in until the differential pressure meter showed that P_{c1} was greater than P_{cs} . This step was found necessary because preliminary tests showed that when the gate valve was closed, P_{cs} was always greater than P_{c1} even with the heater on. Due to the very long waiting time necessary for equilibrium, it was found more convenient to introduce a small quantity of gas in order to balance the initial difference ($P_{cs} - P_{c1}$). The recorder was then started and a trace of this pressure difference was taken for a period of time. This pressure difference initially

usually decreased as some gas molecules started to migrate into the other end of the small tubing. When the recorder indicated that the value of ($P_{cl} - P_{cs}$) had reached a constant, it was assumed that such difference was maintained by thermal transpiration effect. This was taken as the required value of ($P_{cl} - P_{cs}$), or ($P_h - P_{cs}$) if ($P_h - P_{cl}$) was neglected. The absolute pressure P_{cl} was then read from the Alphatron pressure meter. Some additional gas was bled in again and the above procedure was repeated to obtain further experimental points.

4-5 Results

The absolute pressure at the cold end of the large tube P_{cl} , the difference in pressure, $P_{diff} = P_{cl} - P_{cs}$ and the temperatures at the ends of the small tubing T_h and T_c were recorded and tabulated in Tables (4-1) to (4-7). From these values, the pressure at the cold end of the small tube P , the Knudsen number based on the condition at the cold end K_{nc} and finally the pressure ratio P_r were calculated from the following expressions:

$$P_{cs} = P_{cl} - P_{diff} \qquad 4\text{-}1$$

$$K_{nc} = \frac{\lambda}{d}$$

where

$$\lambda = \frac{16}{5\sqrt{2\pi}} \frac{\mu}{P\sqrt{RT}} \qquad \text{(Ref. 10)}$$

For Helium, λ is given by

$$\lambda_{He} = 1725 \frac{\mu\sqrt{T}}{P} \quad \text{in.}$$

and for Argon, λ is given by

$$\lambda_{Ar} = 545 \frac{\mu\sqrt{T}}{P} \quad \text{in.}$$

in which μ is in poise, P in micron mercury, T in $^{\circ}K$.

Thus

$$K_{nc}\Big]_{He} = \frac{17.25\,\mu\sqrt{T_c}}{P_c d}$$

$$K_{nc}\Big]_{Ar} = \frac{545\,\mu\sqrt{T_c}}{P_c d} \qquad 4\text{-}2$$

The values of μ were obtained from Ref.(18)

The pressure ratio P_r is given by

$$P_r = \frac{P_{cs}}{P_h} = \frac{P_{cs}}{P_{c1}} \qquad 4\text{-}3$$

These values, P_{cs} , P_r and K_{nc} are also included in Tables (4-1) to (4-7).

Graphs (1) to (7) show the experimental results as well as the theoretical predictions of equations (3-20) and (3-21).

TABLE 4-1

Experiment No: EX01

Gas: Helium Diameter of small tubing d:0.03"

T_h : 674.5°K T_c : 303°K T_r : 2.226

P_{cl} (μ Hg) Meter reading	Actual value *	P_{diff} (μ Hg)	P_{cs} (μ Hg)	K_{nc}	P_r
165	782	18	764	0.2673	0.9769
230	1090	6	1084	o.1884	0.9944
610	2890	25	2865	0.0713	0.9913
690	3270	28	3242	0.063	0.9914
770	3650	30	3620	0.0564	0.9917
840	3990	34	3956	0.0516	0.9914
910	4310	35	4275	0.0478	0.9918
1100	5210	28	5182	0.0394	0.9946
1430	6870	28	6842	0.0298	0.9959
5000	23700	44.5	23655	0.0086	0.9981
7400	35100	36	35064	0.0058	0.9989

* Since the sensitivity of the Aphatron pressure gauge is different for different gases, the meter reading has to be multiplied by a factor to give the actual value of pressure. The factor is a constant for a particular gas and is given in the instruction booklet for the Alphatron pressure gauge.

TABLE 4-2

Experiment No: EX02

Gas: Helium Diameter of small tubing d=0.03"

T_h : 680 °K T_c : 303 °K T_r=2.244

P_{cl} (μ Hg) Meter reading	Actual value	P_{diff} (μ Hg)	P_{cs} (μ Hg)	K_{nc}	P_r
265	1260	16	1244	0.1641	0.9873
990	4700	80	4620	0.0441	0.9829
1900	9000	82.5	8917.5	0.0228	0.9908
2100	9950	76	9874	0.0206	0.9923
2800	13300	72	13228	0.0154	0.9945
3600	17100	67	17033	0.0119	0.9960
4200	19900	61	19839	0.0102	0.9969
5000	23700	48	23652	0.0086	0.9979
5900	28000	42	27957	0.0073	0.9984
6400	30400	43	30358	0.0067	0.9986

TABLE 4-3

Experiment No: EX03

Gas: Argon Diameter of small tubing d=0.03 in.

T_h : 508 °K T_c : 303 °K T_r =1.677

P_{cl} (μ Hg) Meter reading	Actual value	P_{diff} (μ Hg)	P_{cs} (μ Hg)	K_{nc}	P_r
580	487.2	24	463.2	0.1564	0.9507
760	638.4	30	608.4	0.1190	0.9530
960	806.4	36	770.4	0.0939	0.9553
1500	1260	39.5	1220.5	0.0593	0.9686
1900	1596	45.5	1550.5	0.0467	0.9714
2300	1932	41	1891	0.0382	0.9787
2700	2268	38.5	2229.5	0.0324	0.9830

TABLE 4-4

Experiment No: EX04

Gas: Argon Diameter of small tubing d=0.03 in.

T_h : 684 °K T_c : 314.5 °K T_r : 2.175

P_{c1} (μHg) Meter reading	Actual value	P_{diff} (μHg)	P_{cs} (μHg)	K_{mc}	P_r
570	478.8	38	440.8	0.1718	0.9206
740	621.6	48	675.8	0.1120	0.9247
870	730.8	55	573.6	0.132	0.9228
1900	1596	74	1522	0.0497	0.9536
2250	1890	72	1818	0.0416	0.9619
2650	2226	70	2156	0.0351	0.9686
2950	2478	72	2406	0.0315	0.9709
3400	2856	66	2790	0.0271	0.9769
3700	3108	66	3042	0.0249	0.9788
4300	3612	61	3551	0.0213	0.9831
5700	4788	54	4734	0.016	0.9887

TABLE 4-5

Experiment No: EX05

Gas: Argon Diameter of small tubing d=0.03 in.

T_h : 816°K T_c : 318°K T_r : 2.566

P_{c1} (μHg) Meter reading	Actual value	P_{diff} (μHg)	P_{cs} (μHg)	K_{nc}	P_r
430	361.2	87.5	273.7	0.4013	0.7578
610	512.4	116	396.4	0.2771	0.7736
770	646.8	126	520.8	0.2109	0.8052
960	806.4	148	658.4	0.1668	0.8164
1700	1428	134	1294	0.0849	0.9062
2100	1764	130	1634	0.0672	0.9263
3000	2520	115	2405	0.0457	0.9544
3700	3108	113	2995	0.0367	0.9636
4700	3948	100	3848	0.0285	0.9747
5900	4956	91	4865	0.0226	0.9816
7000	5880	83	5797	0.0189	0.9859

TABLE 4-6

Experiment No: EX06

Gas: Helium Diameter of small tubing d=0.03 in.

T_h : 548.5°K T_c : 302.5°K T_r : 1.813

P_{cl} (μHg) Meter reading	Actual value	P_{diff} (μHg)	P_{cs} (μHg)	K_{nc}	P_r
215	1019.1	5.5	1013.6	0.2013	0.995
282	1336.7	38	1298.7	0.1571	0.9716
365	1736.1	63.2	1666.9	0.1224	0.9635
435	2061.9	81	1980.9	0.103	0.9607
495	2346.3	92.5	2253.8	0.0905	0.9606
560	2654.4	98.0	2556.4	0.0798	0.9631
610	2891.4	100	2791.4	0.0731	0.9654
680	3223.2	105	3118.2	0.0654	0.9674
755	3578.7	108	3470.7	0.0588	0.9698
925	4384.5	110	4274.5	0.0477	0.9749
1150	5451.0	103	5348.0	0.0381	0.9811
2750	13050.	61	12989.	0.0157	0.9953

TABLE 4-7

Experiment No: EX07

Gas: Helium Diameter of small tubing d=0.03 in.

T_h : 807°K T_c : 315°K T_r : 2.562

P_{cl} (μHg) Meter reading	Actual value	P_{diff} (μHg)	P_{cs} (μHg)	K_{nc}	P_r
530.	2512.2	195.	2317.2	0.0925	0.9224
640.	3033.6	210.	2823.6	0.0759	0.9307
700.	3318.	220.	3098.	0.0691	0.9337
800.	3792.	229.	3563.	0.0601	0.9396
915.	4337.1	235.	4102.1	0.0522	0.9458
1100.	5214.	240.	4974.	0.0431	0.954
1450.	6870.	238.	6635.	0.0323	0.9654
2700.	12798.	190.	12608.	0.017	0.9852
5350.	25359.	110.	25249.	0.0085	0.9957

5. DISCUSSIONS AND CONCLUSIONS

As can be seen from Fig. (1), data of experiment no. EX01 deviate greatly from theoretically predicted values. It was suspected that this was due to the fact that insufficient pump down time was allowed for to eliminate outgassing effects. The molecular weight of the gas evolved from the surface of the wall, mainly air, is about seven times that of helium, the gas under test, but the Knudsen number was calculated using the molecular weight of helium. It can be seen from the expression for mean free path that the Knudsen number depends on the value of the gas constant R. Heavier molecules have shorter mean free paths (smaller Knudsen numbers) under the same conditions. This means that the experimental points in Figure (1) should probably be located further to the left where the ratio P_c / P_h is greater. The extent of this effect is unknown because of the difficulty in estimating outgassing.

Results of experiments for argon seem to agree better with theory. This too is supported by the reasoning in the above paragraph since the molecular weight is much closer to that of air than is helium. A slight increase of air into this gas would have a much less serious influence than into helium.

Since Knudsen number is inversely proportional to pressure, it is very sensitive to any change in pressure when the pressure is low. This fact was initially overlooked. It causes the data from the first few experiments to be unevenly distributed, especially in experiments (2) and (4). Most of the data were crowded in the higher pressure (or smaller Knudsen number) range.

Although it was possible to reduce the rate of increase of pressure, when the gate valve GV1 was closed, to about 25 microns mercury per hour, it seems that this rate is still too large for meaningful experiments at higher Knudsen number. This is evident from the fact that most experimental data deviates further at higher Knudsen numbers. However, comparing with the theory in which it is assumed $\sigma=0.8$, it is encouraging that most data do not deviate by more than about 5%. Such a small error is probably allowable since experiments on rarefied gases are plagued by extraneous effects. Tompkin and Wheeler's results (1) which show pressure ratios greater than unity are proof of this. (See figures 13 and 14.)

Knudsen's equation contains a constant k, the value of which is quite uncertain. On the basis of Leob's remarks (4), a value of 2.5 has been assigned to it. Some variation in this value, particularly with Knudsen number, could give rise to substantial differences.

Most experimental data including those of Arney and Bailey (2,6) seem to agree better with theory if a value $\sigma = 0.8$ rather than $\sigma = 1.0$ is selected. This is quite reasonable since it is not likely that gas molecules are totally reflected diffusely.

Figure (8) shows the effect of σ on thermal transpiration. This graph shows that for any value of Knudsen number, pressure ratios tend to unity if σ is zero, i.e. if all the gas molecules are reflected specularly. However, in practice, the value of σ will never reach zero because all surfaces are rough on a microscopic scale. Consequently most gas molecules would be more likely reflected diffusely. The value of σ for most cases will be less but close to unity.

Unfortunately, the highest Knudsen number obtained in the experiments was about 0.2. Attempts were made to conduct experiments at greater Knudsen numbers; however, they were unsuccessful because an amount of gas had to be bled into the system before the first reading could be taken.(As discussed in section 4-4.) This introduced gas would always bring the chamber pressure up to a value around 10^{-1} torr, corresponding to a Knudsen number of about 0.1 based on the tube diameter used. To improve the situation, it is suggested that the pump down time be prolonged so that the initial pressure difference across the small tubing can be reduced. In this way less gas would be required to off-set the initial

pressure difference. Another method is to place a vacuum valve across the two sensing ports of the differential pressure transducer. During the pump down period, this additional valve could be opened allowing gas from the cold end of the small tubing to be pumped out through a larger size of tube.

It is concluded that the present theory developed, equations (3-20) and (3-21), predicts the thermal transpiration effect reasonably well in the slip flow regime. Since it includes σ, the fraction of molecules that are reflected diffusively, it is more general than previous forms due to the fact that it takes into account surface interaction effects. This form would be very useful if the value of σ were known. On the other hand, if one can accurately measure the thermal transpiration effect, equations (3-20) and (3-21) can then be used as a means to determine the value of σ for any gas interacting with any type of surface.

It is also concluded that outgassing effects should be effectively eliminated if meaningful experiments at higher Knudsen numbers are to be conducted.

Finally, it is hoped that although equations (3-20) and (3-21) were derived only for the slip flow regime, they can be modified to cover the much wider regime from slip flow to free-molecule flow. In this way, equations would be available , containing σ as a parameter and governing the whole flow regime.

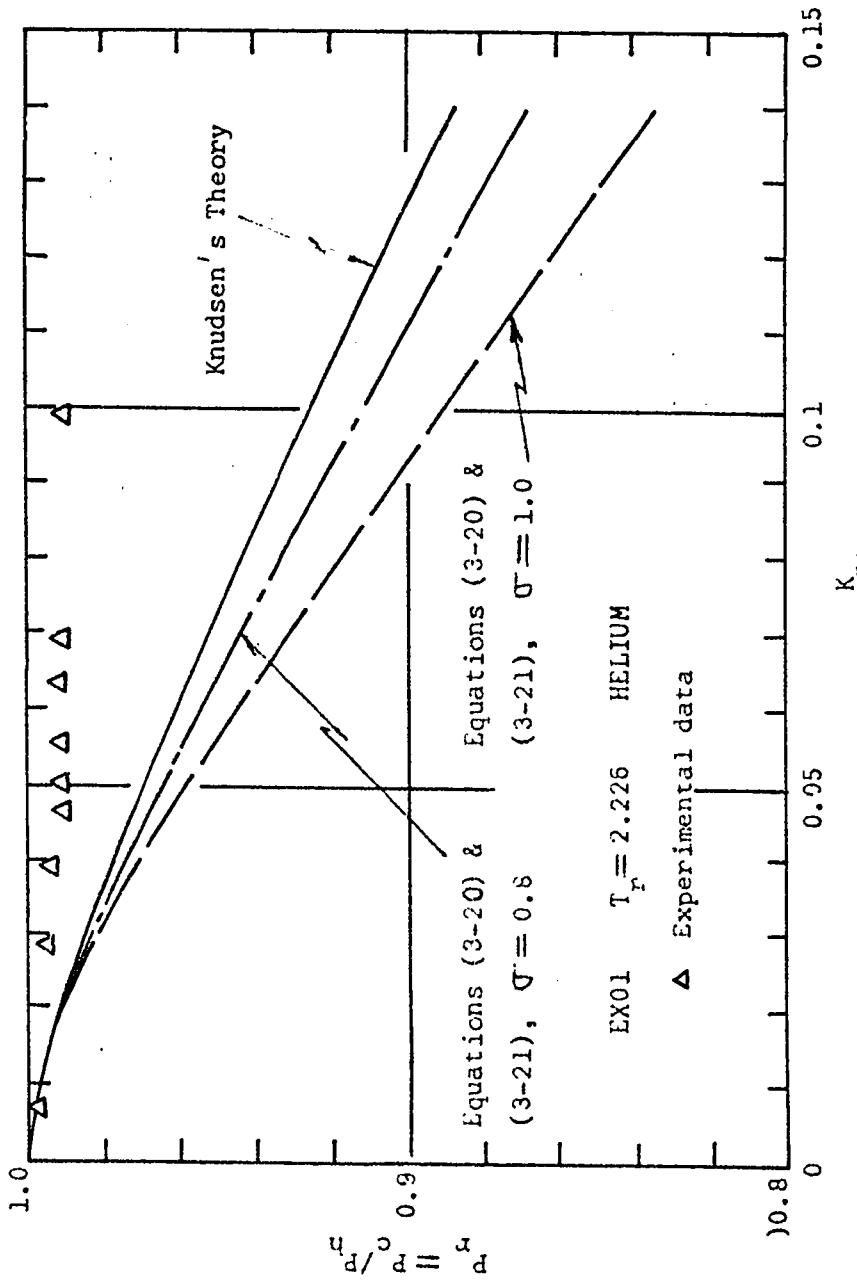

Figure (1) Comparision of experimental data with theory

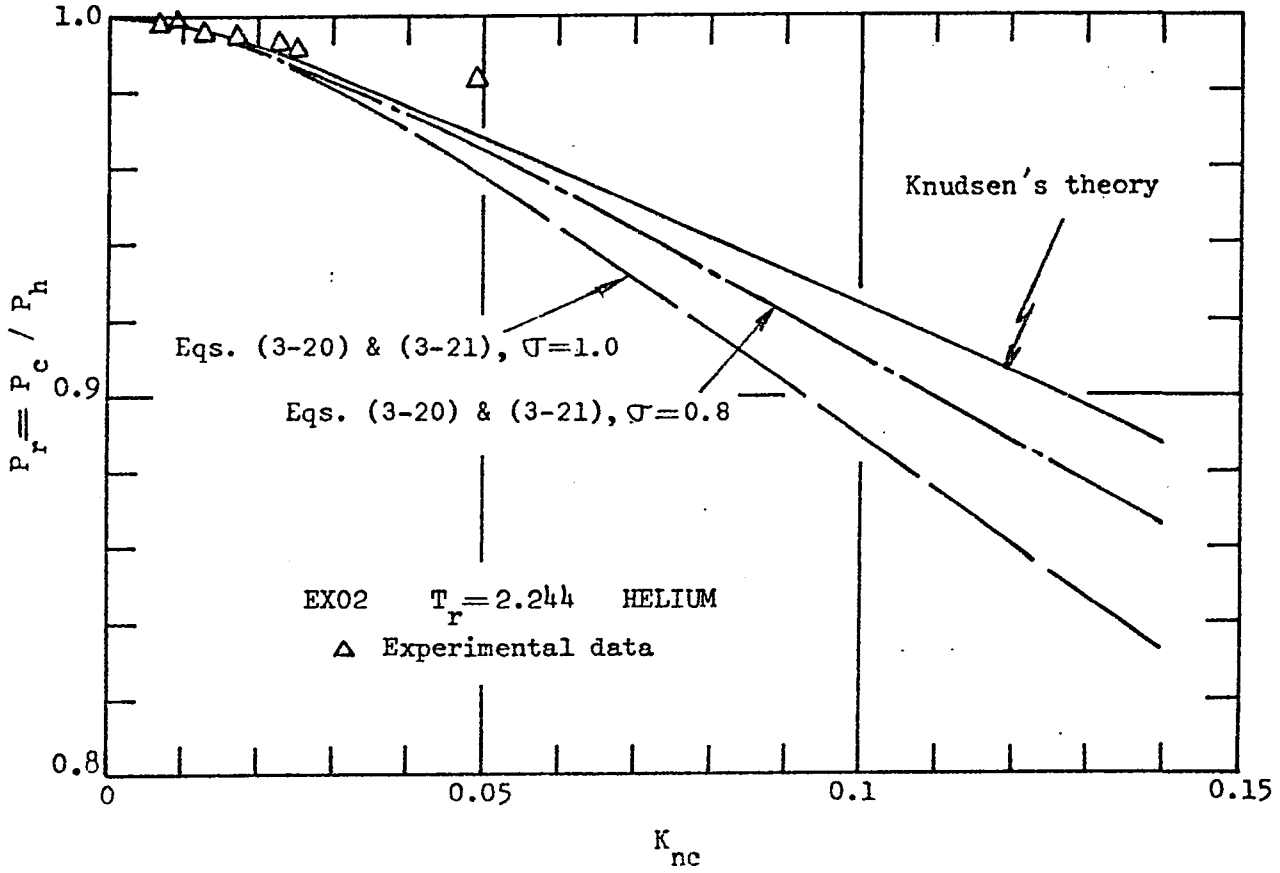

Figure (2) Comparision of experimental results with theory .

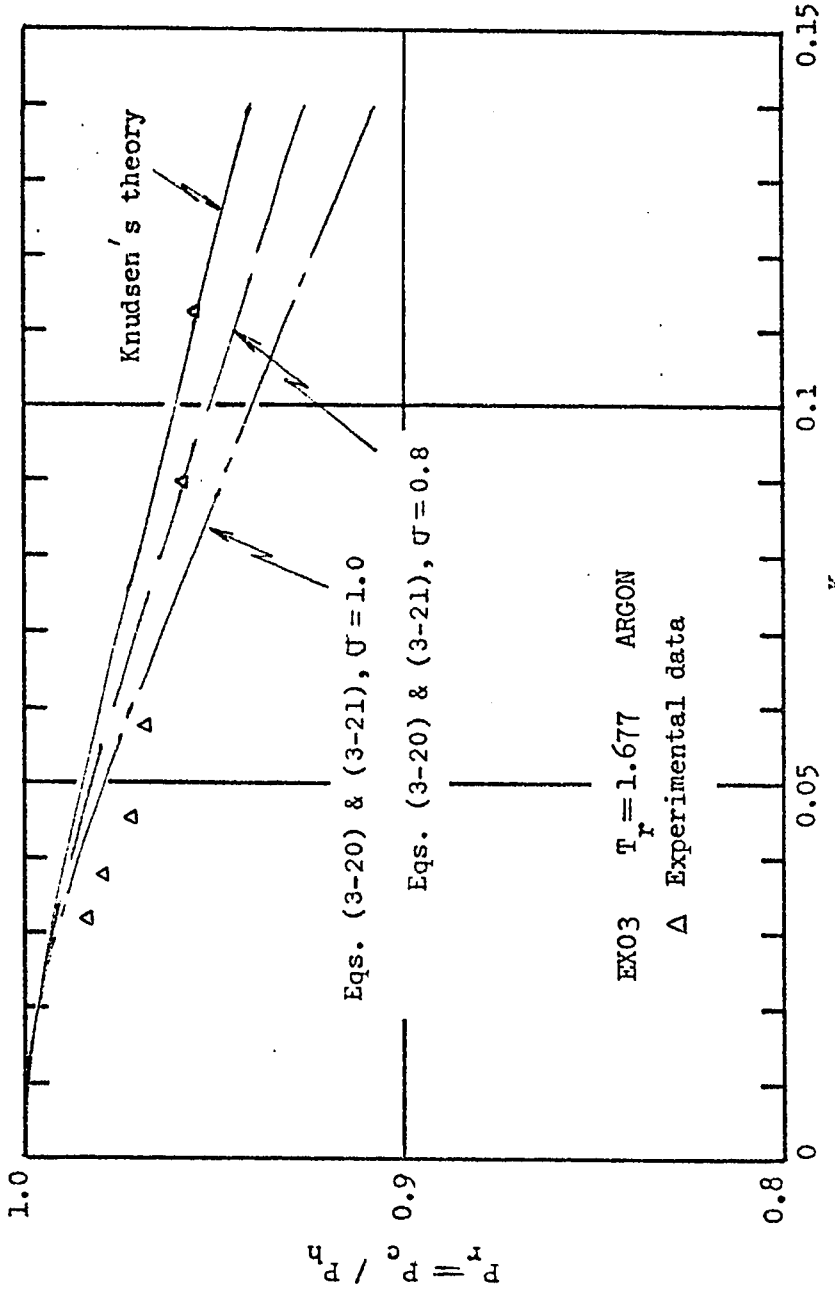

Figure (3) Comparision of experimental results with theory

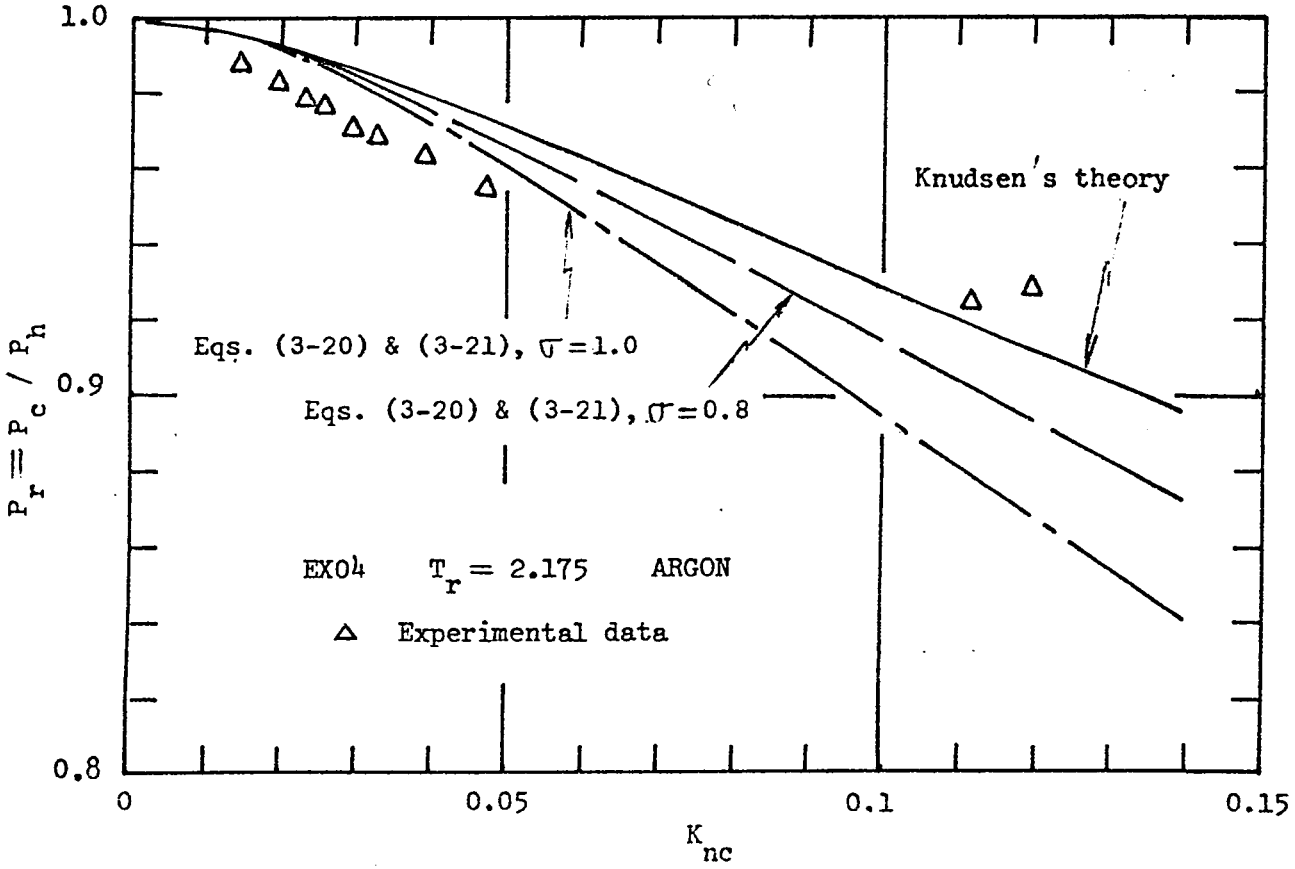

Figure (4) Comparision of experimental results with theory

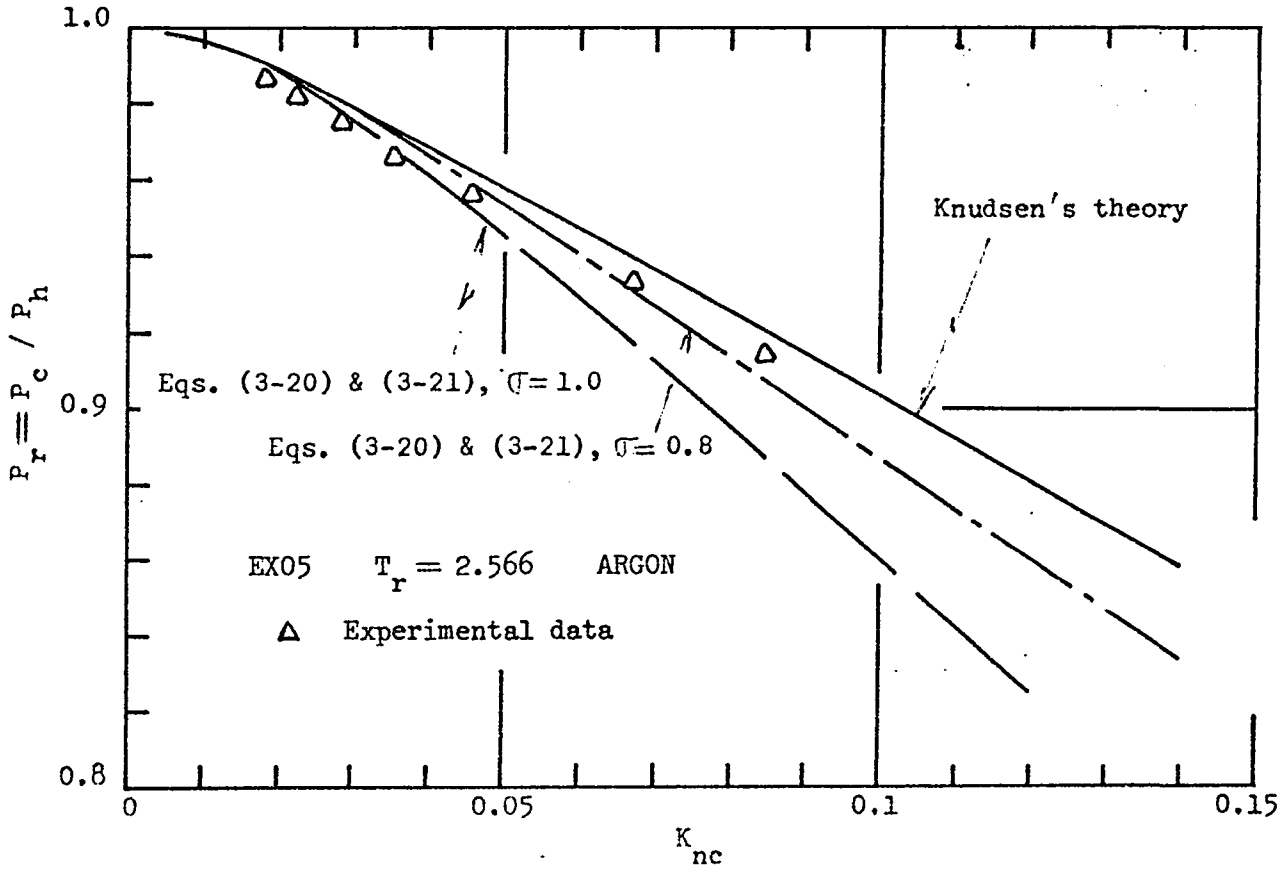

Figure (5) Comparision of experimental data with theory

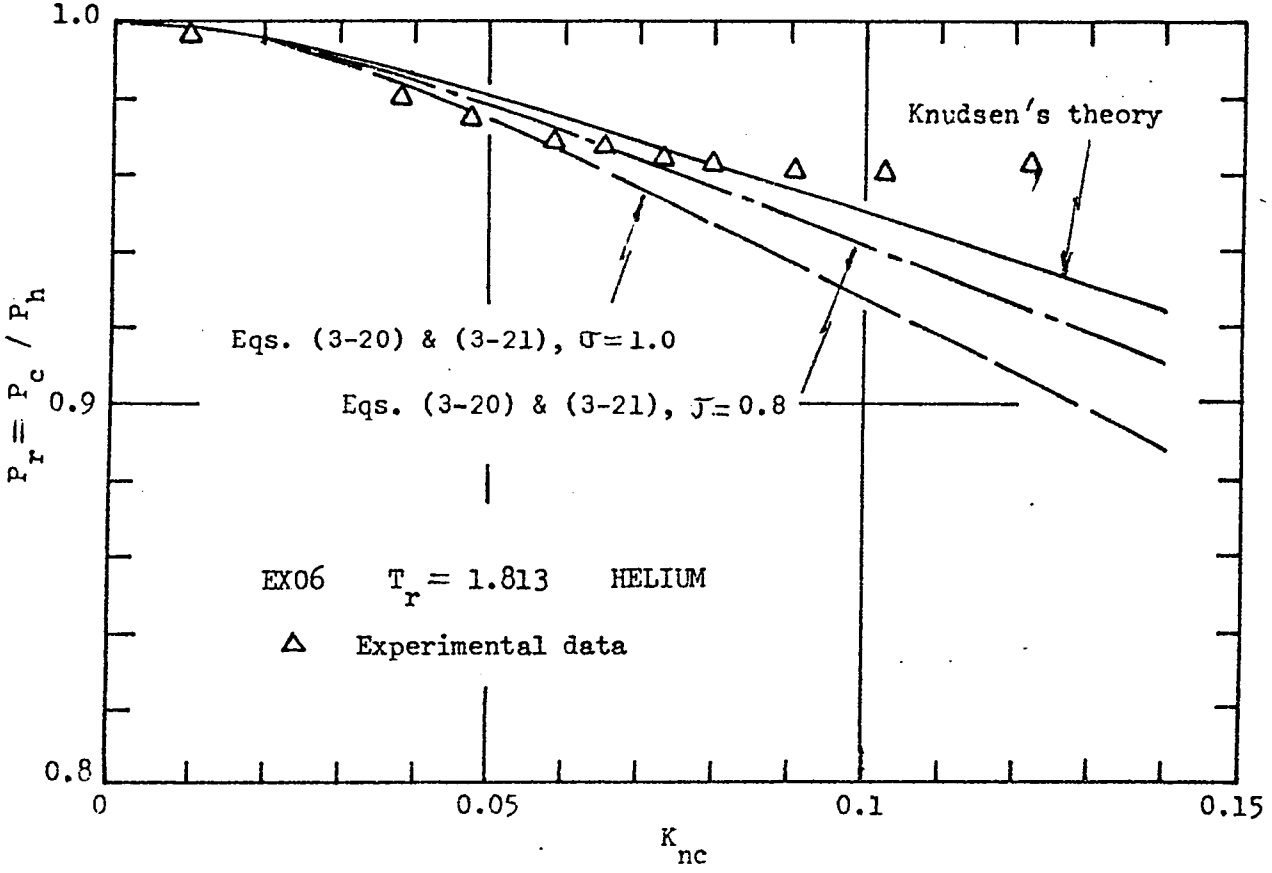

Figure (6) Comparision of experimental results with theory

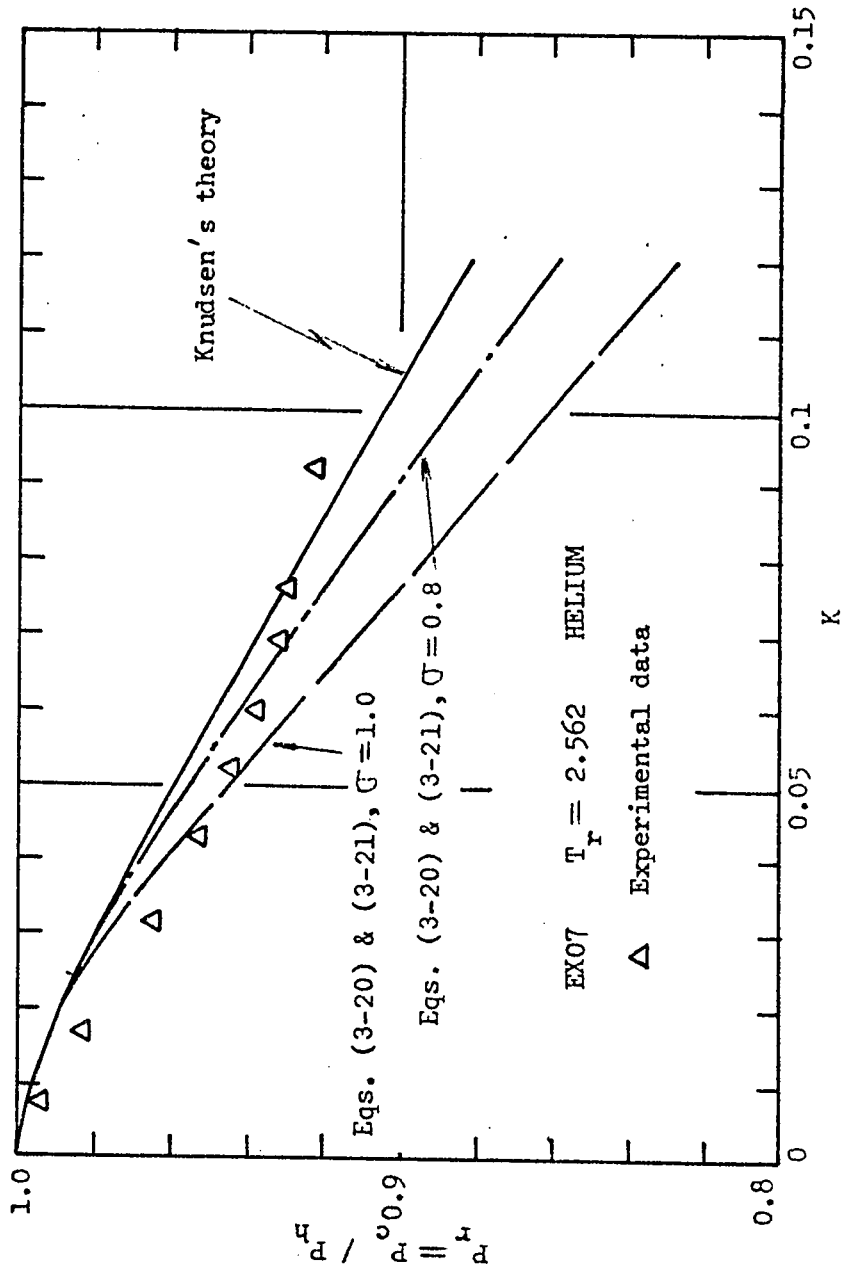

Figure (7) Comparision of experimental results with theory

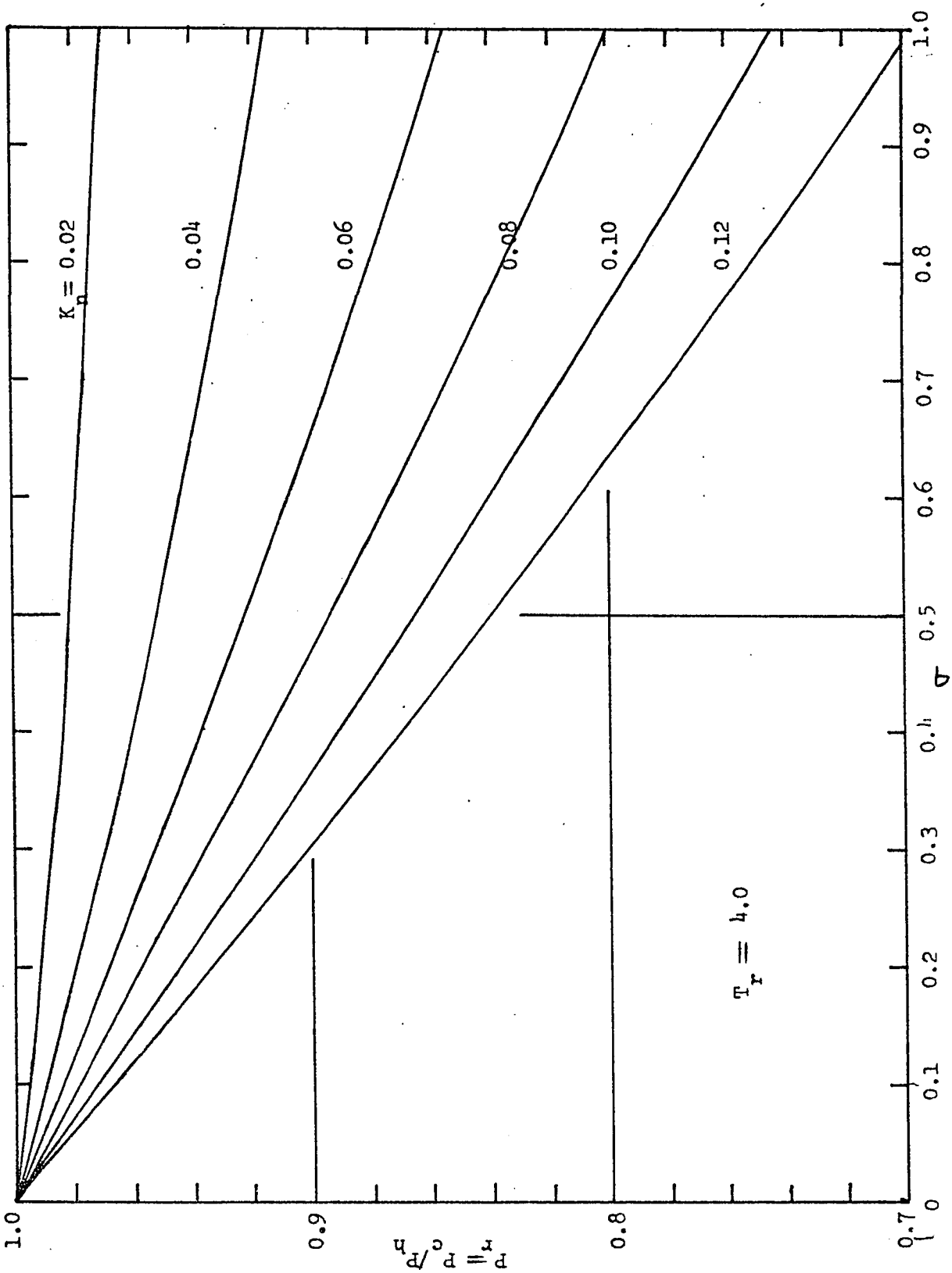

Figure (8) The effect of σ on thermal transpiration

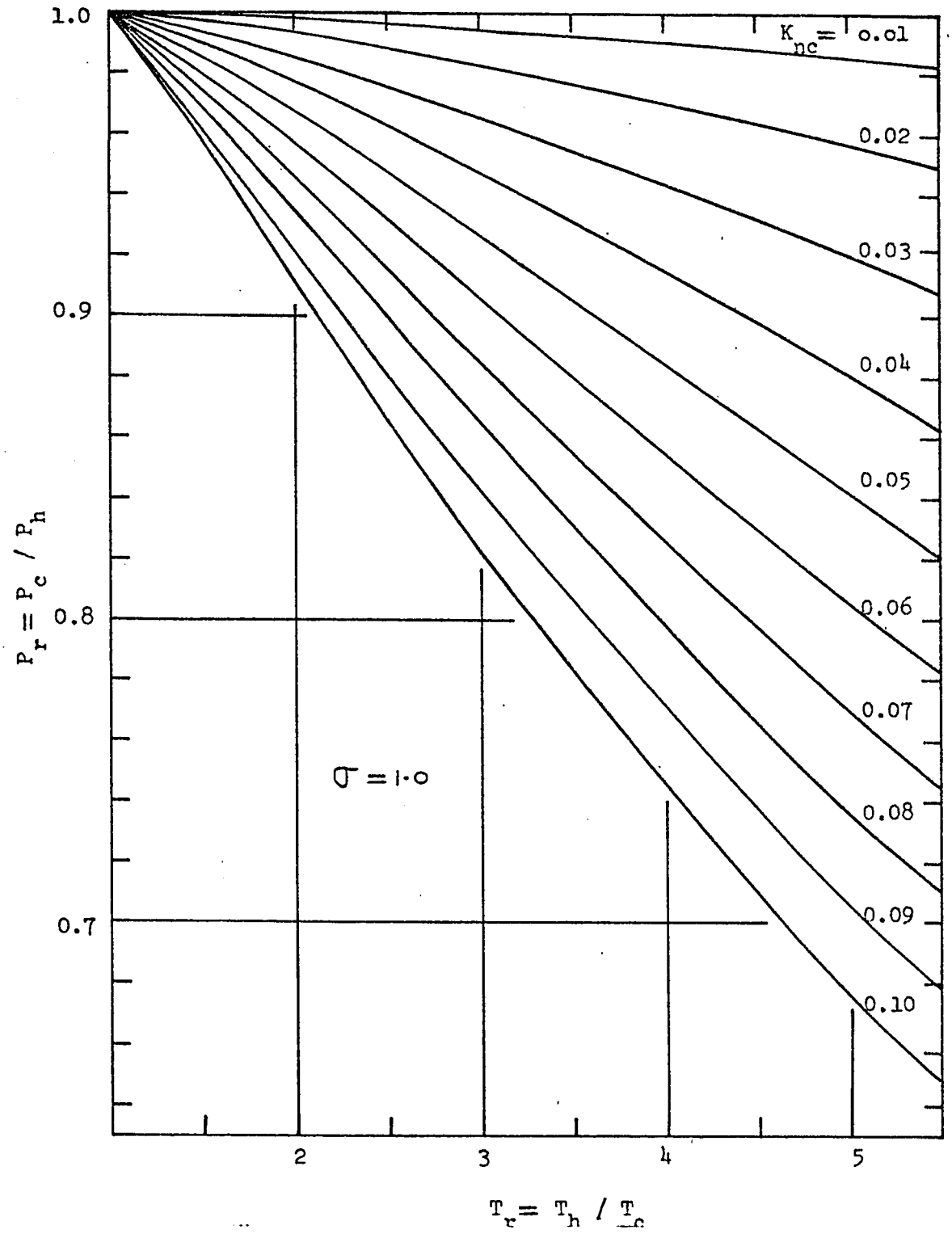

Figure (9) Variation of pressure ratio with temp. ratio, $\sigma = 1.0$

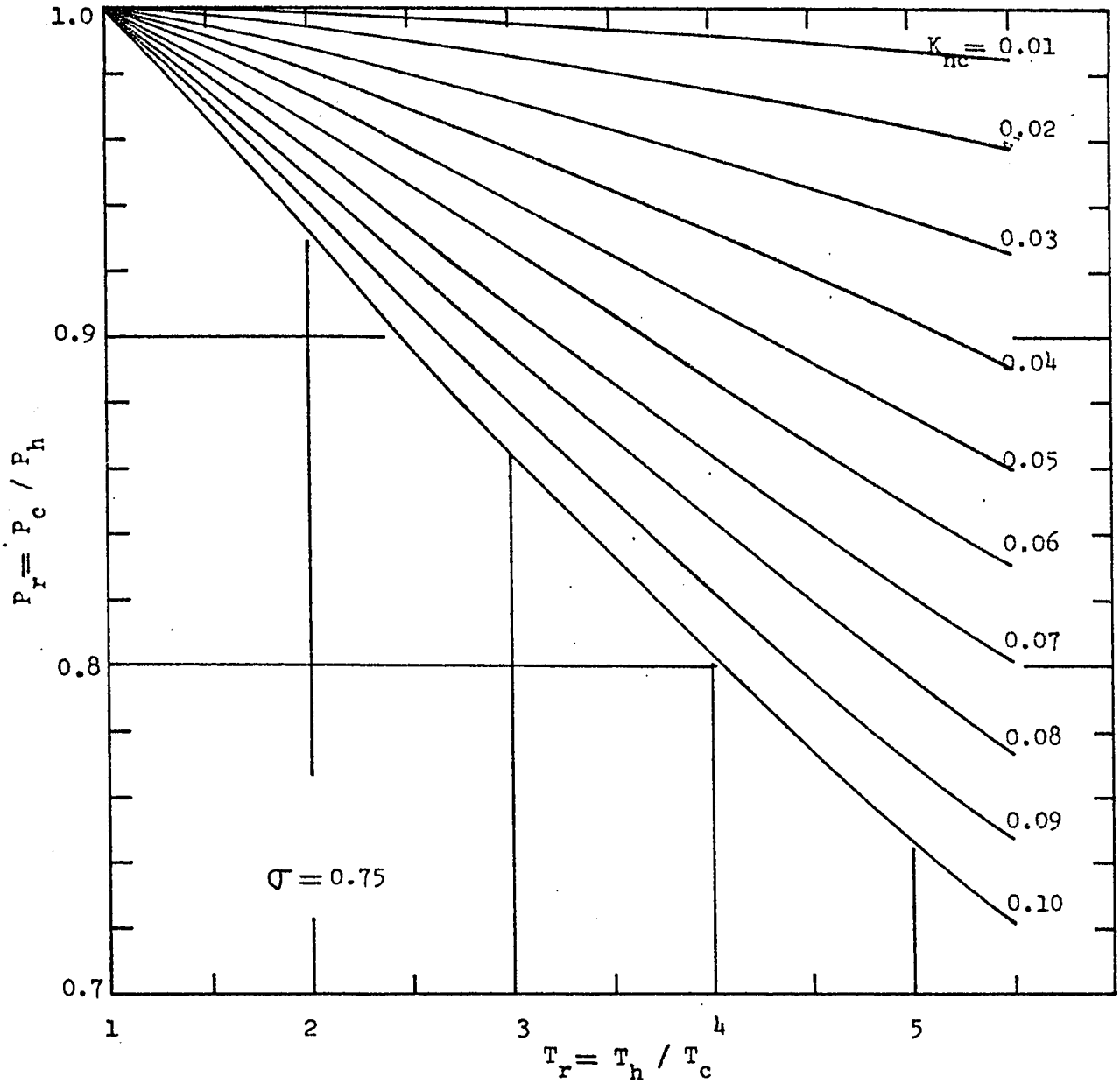

Fig. (10) Variation of pressure ratio with temperature ratio. $\sigma = 0.75$

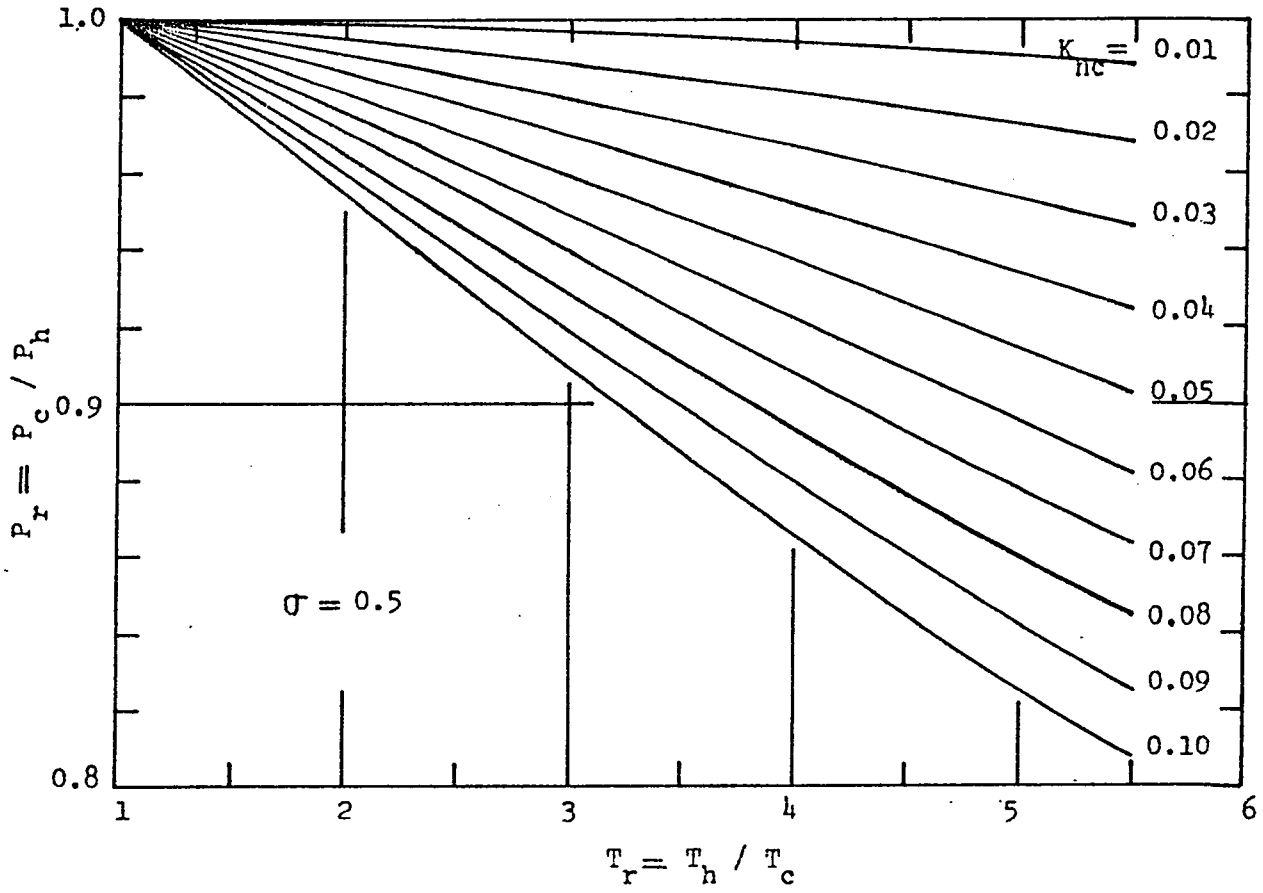

Figure (11) Variation of pressure ratio with temperature ratio. σ=0·5

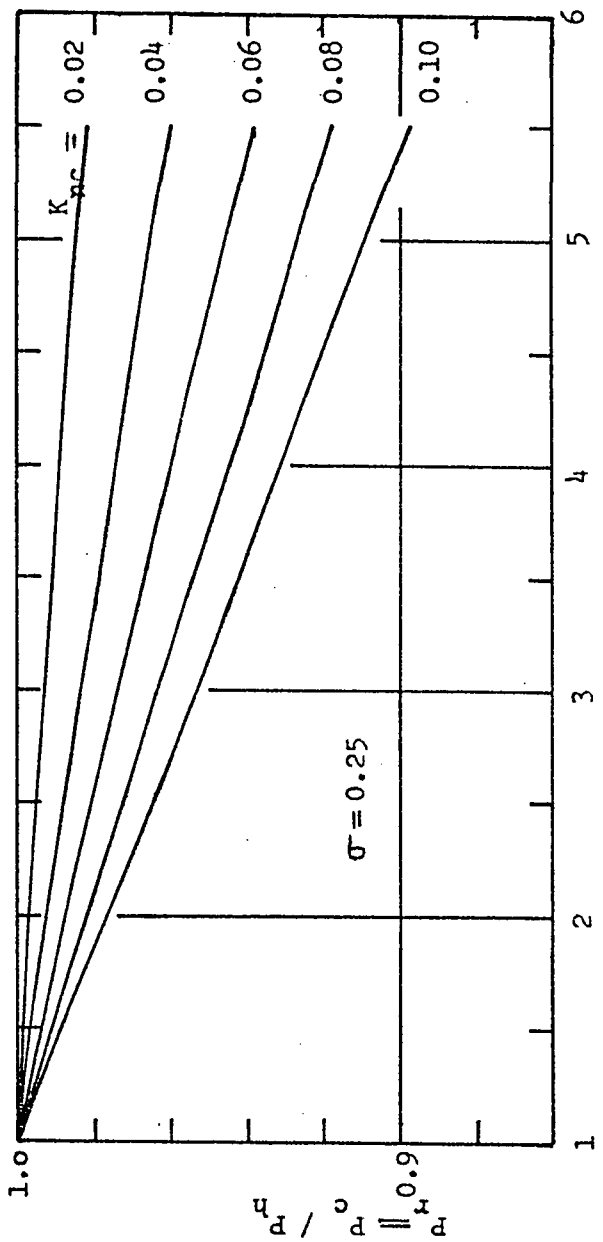

Figure (12) Variation of pressure ratio with temperature ratio. $\sigma = 0.25$

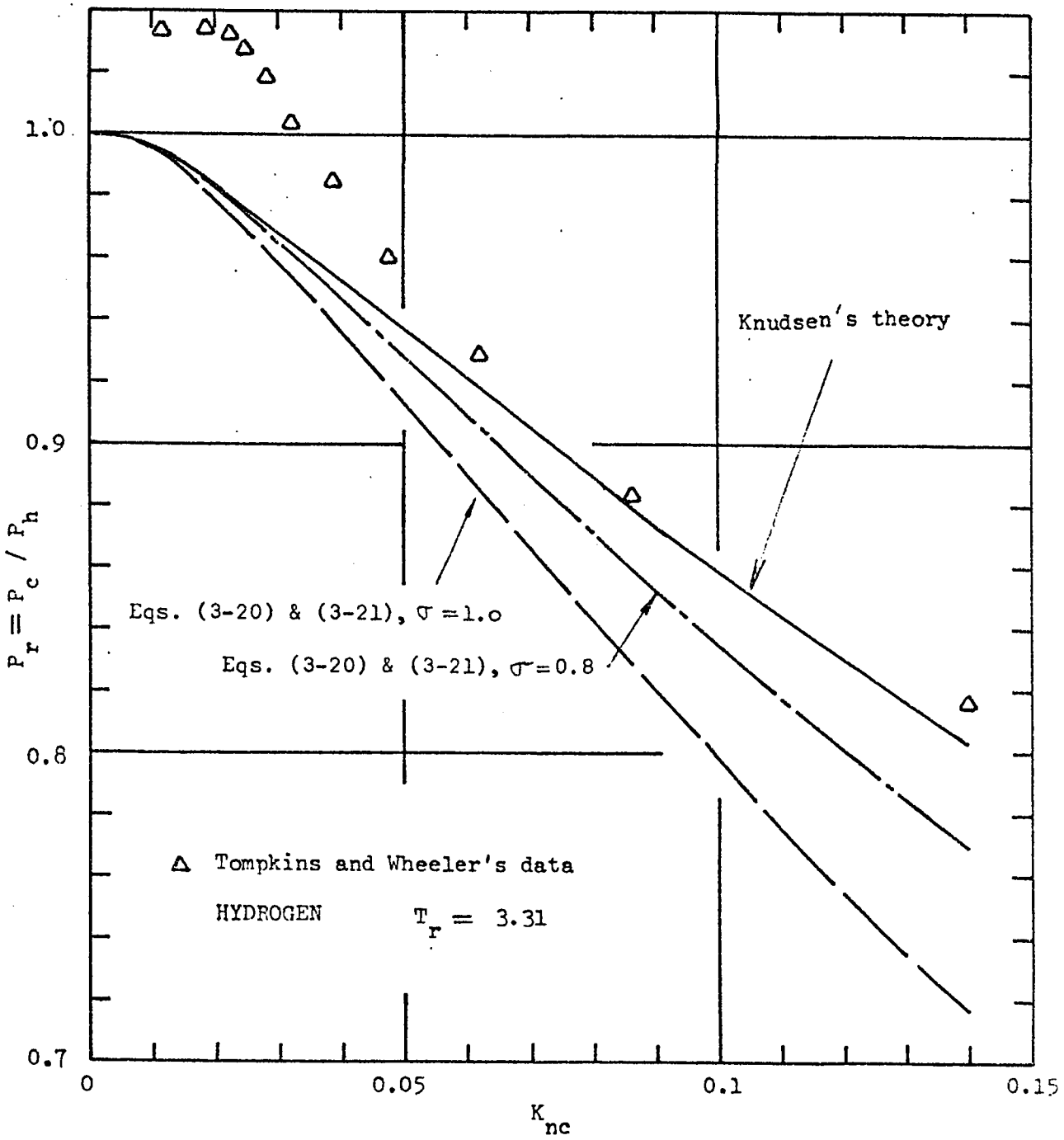

Figure (13) Comparision of Tompkins and Wheeler's result with Theory

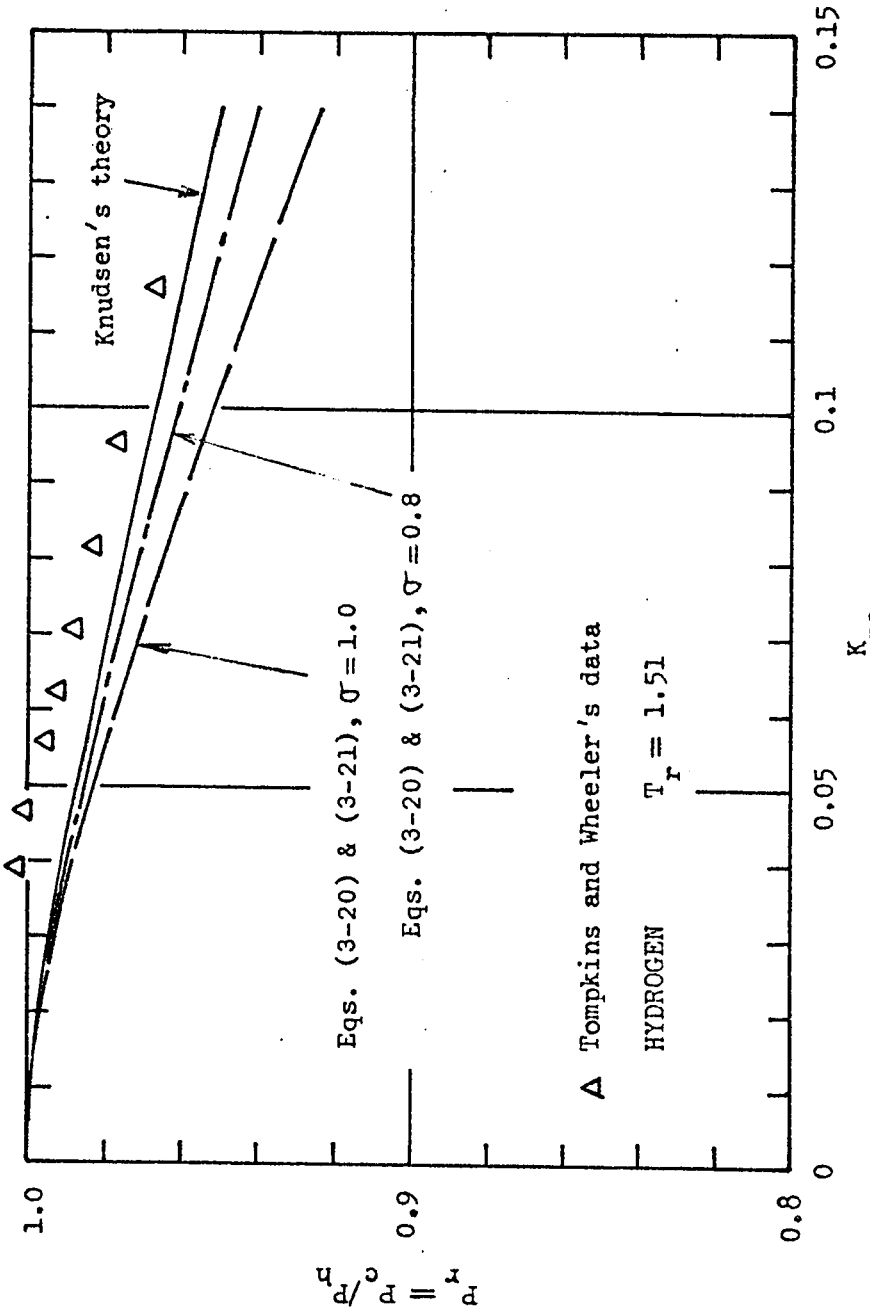

Figure (14) Comparision of Tompkins and Wheeler's result with theory

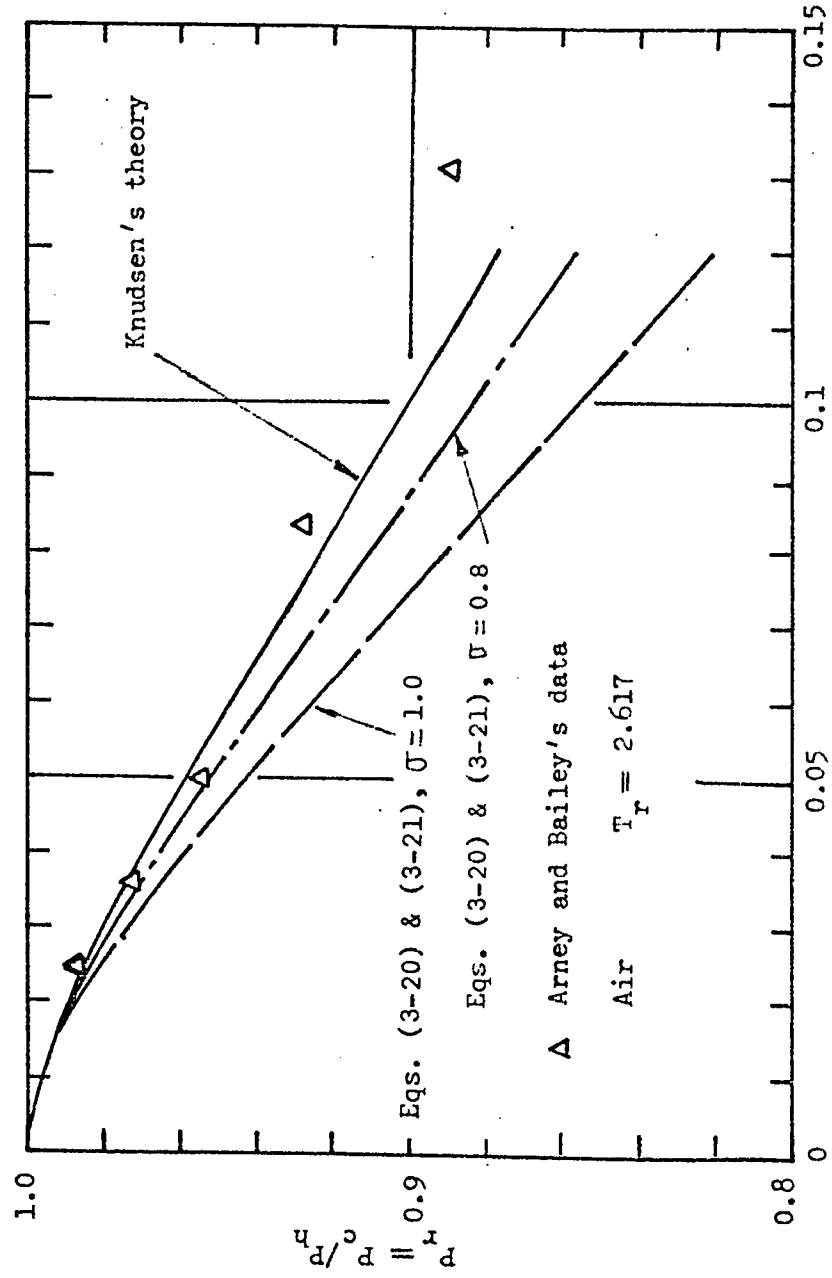

Figure (15) Comparision of Arney and Bailey's experimental data with theory

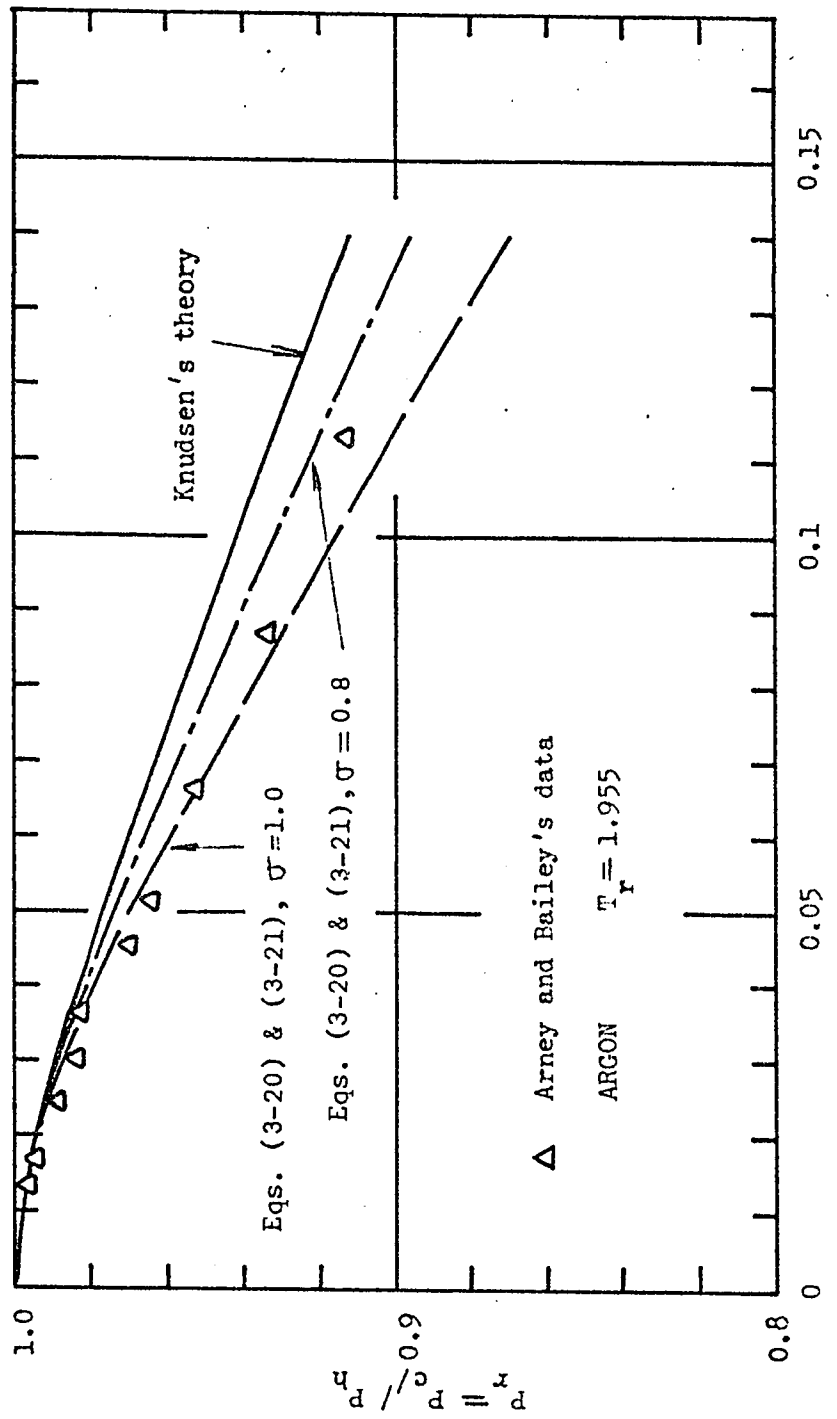

Figure (16) Comparision of Arney and Bailey's experimental data with theory

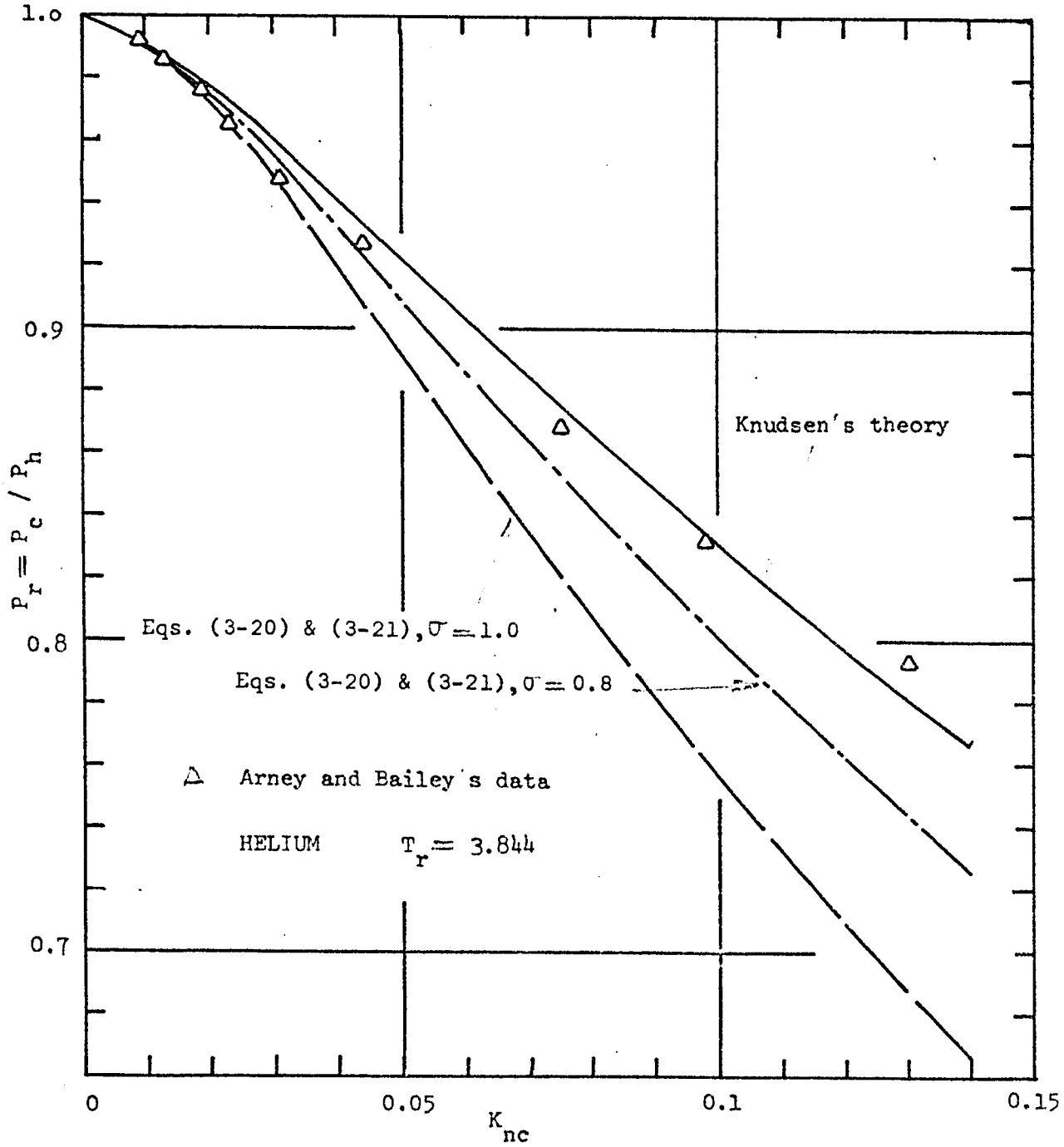

Figure (17) Comparision of Arney and Bailey's experimental data with theory

REFERENCES

1. Tompkins, F.C. Wheeler, D.E. — "The Correction for Thermo-Molecular Flow", Transactions of the Faraday Society, Vol.29, Nov. 1933, pp 1248-1254.

2. Arney, G.D. Jr., Bailey, A.B. — "An Investigation of the Equilibrium Pressure Along Unequally Heated Tubes", AEDC-TDR-62-26, Feb., 1962

3. Knudsen, M. — Kinetic Theory of Gases, John Wiley and Sons, 1952.

4. Loeb, L.B. — The Kinetic Theory of Gases, Dover Publications, Inc. 1961.

5. Liang, S.C. — "Some Measurements of Thermal Transpiration", Journal of Applied Physics, Vol.22, No 2, Feb. 1951, pp 148-153.

6. Arney, G.D. Jr. Bailey, A.B. — "Addendum to an Investigation of the Equilibrium Pressure Along Unequally Heated Tubes", AEDC-TDR-62-188, Oct., 1962.

7. Edmonds, T. Hobson, J.P. — "A Study of Thermal Transpiration Using Ultrahigh Vacuum Techniques", J. Vac. Sci. Technol., No 2, 1965, pp 182-197

8. Kennard, E.H. — Kinetic Theory of Gases, McGraw-Hill Book Comp., Inc. 1938.

9. Lee, J.P. Sears, F.W. Turcotte, D.L. — Statistical Thermodynamics, Addison-Wesley Publishing Co., 1963

10. Patterson, G.N. — Molecular Flow of Gases, John Wiley and Sons, Inc, 1956

11. Bhatnagar, P.L. Gross, E.P. Krook, M. — "A Model for Collision Processes in Gases. I. Small Amplitude Processes in Charged and Neutral One-Component Systems", Phys. Rev., Vol.94, No.3, 1954, pp514-524.

12. Vincenti, W.G. Kruger, C.H. Jr. — Introduction to Physical Gas Dynamics, John Wiley and Sons, 1965

13. Chapman, S. Cowling, T.G. — Mathematical Theory of Non-uniform Gases, Cambridge University Press, 1958.

14. Grad, H. — "On the Kinetic Theory of Rarefied Gases", Communications on Pure and Applied Mathematics, Vol.2, No.231, 1949 pp 331-407

15. Grad, H. — "Theory of Rarefied Gases", Rarefied Gas Dynamics, Proceedings of the 1st International Symposium, Pergamon Press, 1960. pp 100-138

16. Hurlbut, F.C. — "Current Developments in the Study of Gas-Surface Interactions", Rarefied Gas Dynamics, Academic Press, 1967. pp1-48

17. Pai, S.I. — Viscous Flow Theory, Vol.1, Van Nostrand, 1956

18. Svehla, R.A. — "Estimated Viscosities and Thermal Conductivities of Gases at High Temperatures", Technical Report R-132 NASA.

19. Burington, R.S. — Handbook of Mathematical Tables and Formulas, Handbook Publishers, Inc. 1948.

APPENDIX A

INTEGRAL FORMULAE

1. $$f(n) = \int_0^\infty x^n e^{-ax^2} dx$$

n	f(n)	n	f(n)
0	$\frac{1}{2}\sqrt{\frac{\pi}{a}}$	1	$\frac{1}{2a}$
2	$\frac{1}{4}\sqrt{\frac{\pi}{a^3}}$	3	$\frac{1}{2a^2}$
4	$\frac{3}{8}\sqrt{\frac{\pi}{a^5}}$	5	$\frac{1}{a^3}$
6	$\frac{15}{16}\sqrt{\frac{\pi}{a^7}}$	7	$\frac{3}{a^4}$

If n is even,

$$\int_{-\infty}^{\infty} x^n e^{-ax^2} dx = 2 f(n)$$

If n is odd,

$$\int_{-\infty}^{\infty} x^n e^{-ax^2} dx = 0$$

(Ref. 9)

2. $$\int \frac{x\,dx}{ax^2+bx+c} = \frac{1}{2a}\ln(ax^2+bx+c) - \frac{b}{2a}\int \frac{dx}{ax^2+bx+c}$$

$$\int \frac{dx}{ax^2+bx+c} = \frac{1}{\sqrt{b^2-4ac}} \ln \frac{2ax+b-\sqrt{b^2-4ac}}{2ax+b+\sqrt{b^2-4ac}}$$

for $b^2 > 4ac$

(Ref. 19)

APPENDIX B

SOLUTION OF THE BOLTMANN EQUATION BY EXPANSION OF THE DISTRIBUTION FUNCTION IN HERMITE POLYNOMIALS

Following Patterson (10), dimensionless thermal velocities are first introduced.

$$H_i = \left(\frac{3}{\bar{c}^2}\right)^{1/2} c_i$$

The velocity distribution function can then be expanded in terms of Hermite polynomials with $f^{(o)}$ as the first term in the expansion.

$$f = f^{(o)} \sum \frac{1}{n!} a_i^{(n)} H_i^{(n)}$$

$$f = f^{(o)} \left[1 + a_i H_i + \frac{1}{2} a_{ij} H_i H_j + \frac{1}{6} a_{ijk} H_i H_j H_k + \cdots \right] \qquad \text{B-1}$$

$$i, j, k = 1, 2, 3$$

The order of the subscript numbers in a_{ij} , a_{ijk} is immaterial. Thus $a_{23} = a_{32}$, $a_{123} = a_{231} = a_{321}$.

The coefficients in the expansion are obtained by substituting the distribution function into Maxwell's transfer equation.

$$\frac{\partial}{\partial t}(n\overline{Q}) + \frac{\partial}{\partial x_1}(n\overline{u_1 Q}) + \frac{\partial}{\partial x_2}(n\overline{u_2 Q}) + \frac{\partial}{\partial x_3}(n\overline{u_3 Q})$$

$$= \iiint (Q'_a - Q_a) f_a f_b G s \, d\epsilon \, ds \, d\xi_a \, d\xi_b$$

The left hand side of the above equation then contains quantities like

$$\overline{Q} = \overline{u_1 u_2} + \overline{c_1 c_2}, \quad c_1\overline{Q} = \overline{u_1 c_1 c_2} + \overline{u_2 c_1} + \overline{c_1 c_2} \quad \text{etc.,}$$

which can be determined by taking appropriate moments of the distribution function.

Before the right hand side of the above equation can be integrated it is necessary to first obtain expressions relating particle velocities before and after collision. This process is complicated and requires knowledge of molecular encounters.

When the coefficients of the Hermite polynomials obtained by the above method are substituted into equation (B-1), the distribution function is then found. These coefficients have been calculated by Patterson (10) in detail. Some of the results necessary for the present study are quoted below.

$$Q_{ii} = 0 \qquad \text{B-2}$$

$$2Q_i + Q_{ijj} = 0 \qquad \text{B-3}$$

$$a_{12} = -\frac{\mu}{mn\left(\frac{\overline{c^2}}{3}\right)}\left(\frac{\partial \bar{u}_2}{\partial x_1} + \frac{\partial \bar{u}_1}{\partial x_2}\right) \qquad \text{B-4}$$

$$a_{22} = \frac{2\mu}{mn\left(\frac{\overline{c^2}}{3}\right)}\left[\frac{1}{3}\left(\frac{\partial \bar{u}_1}{\partial x_1} + \frac{\partial \bar{u}_2}{\partial x_2} + \frac{\partial \bar{u}_3}{\partial x_3}\right) - \frac{\partial \bar{u}_2}{\partial x_2}\right] \qquad \text{B-5}$$

$$a_1 = \frac{15\mu}{4mn}\left(\frac{\overline{c^2}}{3}\right)^{-3/2}\frac{\partial}{\partial x_1}\left(\frac{\overline{c^2}}{3}\right) \qquad \text{B-6}$$

APPENDIX C

INTEGRATION OF EQUATION (3-19)

Equation (3-19) is repeated below.

$$\frac{dT}{T} = \frac{\frac{4}{5}\frac{2-\sigma}{\sigma}K_n + \frac{8}{25\pi}}{K_n\left[-1.5\,K_n^2 + \frac{4}{5}\frac{2-\sigma}{\sigma}K_n + \frac{8}{25\pi}\right]} \qquad 3\text{-}19$$

Put $-1.5 = A$, $\frac{4}{5}\frac{2-\sigma}{\sigma} = B$, $\frac{8}{25\pi} = C$.

Equation (3-19) then becomes

$$\frac{dT}{T} = \frac{BK_n + C}{K_n(AK_n^2 + BK_n + C)}\,dK_n$$

The above equation can be intergrated by first separating into partial fractions.

Let $$\frac{BK_n + C}{K_n(AK_n^2 + BK_n + C)} = \frac{D_1}{K_n} + \frac{D_2 + D_3K_n}{(AK_n^2 + BK_n + C)}$$

Multiplying both sides by $K_n(AK_n^2 + BK_n + C)$ and equating like powers of K_n, one obtains

$$C = CD_1$$

$$B = BD_1 + D_2$$

$$0 = AD_1 + D_3$$

From which,

$$D_1 = 1$$

$$D_2 = 0$$

$$D_3 = -A$$

Thus equation (3-19) becomes

$$\int_{T_c}^{T_h} \frac{dT}{T} = \int_{K_{nc}}^{K_{nh}} \left[\frac{1}{K_n} - \frac{AK_n}{AK_n^2 + BK_n + C} \right] dK_n$$

Integrating the above equation with the help of the integral formula in Appendix A,

$$\frac{T_h}{T_c} = \frac{K_{nh}}{K_{nc}} \left[\frac{AK_{nh}^2 + BK_{nh} + C}{AK_{nc}^2 + BK_{nc} + C} \right]^{-\frac{1}{2}} \left[\frac{(2AK_{nh} + B - D)(2AK_{nc} + B + D)}{(2AK_{nh} + B + D)(2AK_{nc} + B - D)} \right]^{\frac{B}{2D}}$$

where $$D = \sqrt{B^2 - 4AC}$$

```
C
C
C     COMPUTER PROGRAME TO SOLVE EQUATIONS (3-20) AND (3-21)
C
C
C     S: THE FRACTION OF MOLECULES DEFLECTED DIFFUSIVELY
C     AKC: KNUDSEN NUMBER AT THE COLD END
C     AKH, FKH: KNUDSEN NUMBER AT THE HOT END
C     TR: TEMPERATURE RATIO, TH/TC
C     PR: PRESSURE RATIO, PC/PH
C     I: NUMBER OF ITERATION
C
C
      WRITE(3,20)
   20 FORMAT(1H1,' VARIATION OF PRESSURE RATIO WITH TEMPERATURE RATIO FO
     1R KNUDSEN NUMBERS AT THE COLD END  FROM 0.01 TO 1.')
      S=1.
      A=-1.5
      B=0.8*(2.-S)/S
      C=8./(25.*3.1416)
      D=(B**2.-4.*A*C)**0.5
      AKC=0.
C
C     DO LOOP 2 ( CHANGE OF KNUDSEN NO AT COLD ) BEGINS
C
  510 AKC=AKC+0.01
      TR=1.
      AKH=AKC
C
C     DO LOOP 1 ( CHANGE OF TEMPERATURE RATIO ) BEGINS
C
  410 TR=TR+0.5
C
```

```
C
C
C      TRIAL AND ERROR BEGINS
C
       I=0
       FKH=AKH
 1000  AKH=AKC*TR*((A*FKH**2.+B*FKH+C)/(A*AKC**2.+B*AKC+C))**0.5/
      1(((2.*A*FKH+B-D)*(2.*A*AKC+B+D))/((2.*A*FKH+B+D)*(2.*A*AKC
      2+B-D)))**(B/(2.*D))
       DIFF=ABS(AKH-FKH)
       R=AKH/1000.
       IF(DIFF-R)310,310,320
  320  FKH=AKH
       I=I+1
       GO TO 1000
C
C      TRIAL AND ERROR ENDS
C
  310  PR=AKH/(TR*AKC)
       WRITE(3,10)S,AKC,TR,PR,AKH,I
   10  FORMAT(/,3X,'S=',F4.2,5X,'KNUDSEN NO AT THE COLD END=',F4.2,5X,'TE
      1MP RATIO=',F3.1,5X,'PRESSURE RATIO =',F8.6,5X,'KN AT HOT END=',F6.
      24,5X,'I=',I3)
        IF(TR-6.)410,410,420
C
C      DO LOOP 1 ENDS
C
  420  IF(AKC-0.3)510,510,520
C
C      DO LOOP 2 ENDS
C
  520  RETURN
       END
```